Design of Computationally Efficient Interpolated FIR Filters

TAPIO SARAMÄKI, YRJÖ NEUVO, SENIOR MEMBER, IEEE, AND
SANJIT K. MITRA, FELLOW, IEEE

Abstract —The number of multipliers required in the implementation of interpolated FIR filters of the form $H(z) = F(z^L)G(z)$ is studied. Both single-stage and multistage implementations of $G(z)$ are considered. Optimal decompositions requiring fewest number of multipliers are given for some representative low-pass cases. An efficient algorithm for designing these filters is described. It is based on iteratively designing $F(z^L)$ and $G(z)$ using the Remez multiple exchange algorithm until the difference between the successive stages is within the given tolerance limits. A novel implementation for $G(z)$ based on the use of recursive running sums is given. The design of this class of filters is converted into another design problem to which the Remez algorithm is directly applicable. The results show that the proposed methods result in significant improvements over conventional multiplier efficient implementations of FIR digital filters.

I. INTRODUCTION

FINITE impulse response (FIR) filters are known to have some very desirable features like guaranteed stability, absence of limit cycles, and linear phase, if desired. The major drawback is the large number of arithmetic operations required in the implementation. The number of multipliers required is, approximately, equal to or half of the length of the filter in the nonlinear and linear phase cases, respectively. The minimum length of the linear phase low-pass FIR filter to meet the frequency domain specifications is approximately

$$N = \frac{-20\log_{10}\sqrt{\delta_p\delta_s} - 13}{14.6\Delta F} + 1 \qquad (1)$$

where δ_p and δ_s are the passband and stopband ripples, and ΔF is the transition bandwidth [1]. The above estimate is rather accurate when the passband and stopband ripples are small. If the ripples are large, a more accurate estimate is given by the more complicated expression in [2].

Several authors [3]–[13] have observed that by letting the filter length increase slightly from the minimum, there can be significant savings in the number of multipliers

and, with some methods, also in the number of adders. This is due to the fact that optimal FIR filters are in a way too general structures to implement typical frequency selective filters. In the direct form implementation, each multiplier determines the value of one impulse response sample independently of the other samples. In the linear phase implementation, the same is true for approximately half of the impulse response values. However, in practical frequency selective filters there is a relatively strong correlation between neighboring impulse response values. By developing filter structures that exploit this correlation, the number of multipliers required in the implementation can be reduced.

In a recent paper, Neuvo, Dong, and Mitra [12] introduced a FIR structure composed of a cascade of FIR filters:

$$H(z) = F(z^L)G(z). \qquad (2)$$

$F(z^L)$ has a periodic frequency response with period $2\pi/L$ and is designed to perform passband, transition band, and stopband shaping in the vicinity of the passband. $F(z^L)$ can thus be called the shaping filter. Because of the periodicity of the response of $F(z^L)$, it has extra unwanted passbands. $G(z)$ is designed to attenuate these extra passbands below the specified maximum stopband level. $G(z)$ is called the interpolator section as it performs time domain interpolation to the sparse impulse response sequence of the shaping filter. The overall realizations are called Interpolated Finite Impulse Response (IFIR) filters. In [12], it was shown that the structure in favorable cases reduces the number of multipliers and adders by almost a factor of L. In addition, roundoff noise and coefficient sensitivities improve.

The IFIR filter is a single-rate structure which is mathematically closely related to signal decimation by a decimator followed by filtering at the lower rate. In the IFIR approach the savings are obtained by interpolating the impulse response and in the decimation approach by decimating the input signal to the filter. These are dual operations in the sense that both approaches make the basic filter to have wider passband and transition band regions with respect to the signal sampling rate and according to (1) the required filter length decreases. Note that as the IFIR structure is a single-rate structure, there can never be internal aliasing problems.

In the design of IFIR filters, one central parameter to be selected is the interpolation factor L. As L is increased, the complexity of the shaping filter decreases but the complexity of the interpolator increases. Note that in the design of decimators the decimation ratio is not generally a free design parameter. In [12], the design of IFIR filters was based on the use of simple interpolators. However, for more stringent filter specifications, this approach is ineffective.

In this paper, we show how the overall IFIR structure including the shaping filter, interpolator, and L can be optimized to arrive at the smallest number of required multipliers. Both single-stage and multistage implementations of $G(z)$ are discussed. The method is based on alternately designing the shaping filter and the interpolator using the Remez multiple exchange algorithm. We also derive approximate expressions that assist in finding the optimal lengths of the subfilters as well as the optimal value of L. In addition to lowpass designs, the proposed approach is equally well applicable to design of high-pass, bandpass, and bandstop filters. The number of multipliers required by low-pass IFIR filters can be further reduced by developing interpolator structures that utilize the fact that the stopbands of the interpolator are equally spaced. One such structure based on the use of recursive running sums is advanced. Finally, the optimal IFIR filters are compared with other known multiplier efficient FIR filter implementations. The results show that among the single-rate structures the proposed approach is quite efficient. Multirate FIR implementations tend to have smaller multiplication rates but require ore multipliers and longer overall delays.

II. DESIGN OF OPTIMAL IFIR FILTERS

A. Transfer Function Decomposition

Let the transfer function of a linear-phase FIR filter be of the form

$$H(z) = F(z^L)G(z) \tag{3a}$$

where

$$G(z) = G_1(z)G_2(z^{L_1})G_3(z^{L_1L_2}) \cdots G_K(z^{L_1L_2\cdots L_{K-1}}) \tag{3b}$$

$$F(z) = \sum_{n=0}^{N_F} f(n)z^{-n} \tag{3c}$$

$$G_i(z) = \sum_{n=0}^{N_{G_i}} g_i(n)z^{-n}. \tag{3d}$$

Here L_i's are selected such that

$$L_K = \frac{L}{L_1L_2\cdots L_{K-1}} \tag{3e}$$

is an integer. Alternatively, $G(z)$ can be expressed in the form

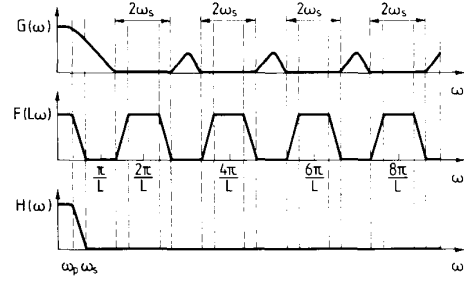$$G(z) = \prod_{i=1}^{K} G_i(z^{L_i}) \tag{4a}$$

Fig. 1.   The specifications for the shaping filter $F(z^L)$ and the interpolator $G(z)$ to meet the overall criteria.

where

$$\tilde{L}_1 = 1, \qquad \tilde{L}_r = \prod_{k=1}^{r-1} L_k, \qquad r = 2,3,\cdots,K. \tag{4b}$$

The zero-phase frequency response of the overall filter can then be written as

$$H(\omega) = F(L\omega)G(\omega) \tag{5a}$$

where

$$G(\omega) = G_1(\tilde{L}_1\omega)G_2(\tilde{L}_2\omega)\cdots G_K(\tilde{L}_K\omega). \tag{5b}$$

Here $F(L\omega)$ denotes the zero-phase response of $F(z^L)$ and $G_i(\tilde{L}_i\omega)$ the response of $G_i(z^{\tilde{L}_i})$.

B. Approximation Problem

Let the specifications of the composite filter be

$$1 - \delta_p \le F(L\omega)G(\omega) \le 1 + \delta_p \text{ for } \omega \in [0,\omega_p] \tag{6a}$$

$$-\delta_s \le F(L\omega)G(\omega) \le \delta_s \text{ for } \omega \in [\omega_s,\pi]. \tag{6b}$$

Since the response $F(L\omega)$ is periodic with period of $2\pi/L$, $[0,\pi/L]$ is the largest interval where the Haar conditions are satisfied and which includes the zero frequency. Therefore, the design of $F(z^L)$ is centered on this interval. It is determined such that the overall filter meets the passband specifications of (6a) and the stopband specifications of (6b) on the subinterval $[\omega_s,\pi/L]$. The requirements for $F(z^L)$ can be stated in terms of $F(\omega)$, the zero-phase response of $F(z)$, as follows:

$$1 - \delta_p \le F(\omega)G(\omega/L) \le 1 + \delta_p, \text{ for } \omega \in [0, L\omega_p] \tag{7a}$$

$$-\delta_s \le F(\omega)G(\omega/L) \le \delta_s, \text{ for } \omega \in [L\omega_s,\pi]. \tag{7b}$$

Because of the periodicity, $F(L\omega)$ has extra undesired passbands centered at $\omega = 2\pi k/L$ for $k = 1,2,\cdots\lfloor L/2\rfloor.$[1] The desired attenuation is not achieved on the following multiband frequency region (see Fig. 1):

$$\Omega_s = \bigcup_{k=1}^{\lfloor L/2\rfloor} \left[k\frac{2\pi}{L} - \omega_s, \min\left(k\frac{2\pi}{L} + \omega_s, \pi\right)\right]. \tag{8}$$

Therefore, $G(z)$ is determined to provide enough attenuation on this region (see Fig. 1). The requirements for

---

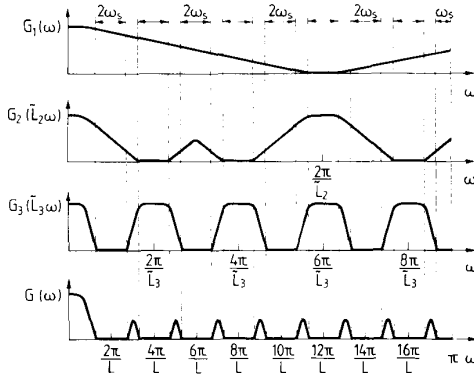[1] $\lfloor x \rfloor$ stands for integer part of x.

Fig. 2. Design of a three-stage ($K = 3$) interpolator $G(z)$ with $L = 18$. $L_1 = L_2, L_3 = 3, \tilde{L}_1 = 1, \tilde{L}_2 = 3, \tilde{L}_3 = 9$.

$G(\omega)$ can be stated as[2],[3]

$$G(0) = 1 \qquad (9a)$$

$$-\delta_s \le F(L\omega)G(\omega) \le \delta_s, \qquad \text{for } \omega \in \Omega_s. \qquad (9b)$$

In the case of the multistage implementation, the desired $G(z)$ can be obtained by determining each one of the subfilters $G_i(z^{\tilde{L}_i})$, $i = 1, 2, \cdots, K$, in such a way that the response $G_i(\omega)$ satisfies

$$G_i(0) = 1 \qquad (10a)$$

$$-\delta_s \le \left[F\left(\frac{L\omega}{\tilde{L}_i} \right) \prod_{\substack{k=1 \\ k \ne i}}^{K} G_k \left(\frac{\tilde{L}_k \omega}{\tilde{L}_i} \right) \right] G_i(\omega) \le \delta_s \qquad \text{for } \omega \in \tilde{\Omega}_i \qquad (10b)$$

where

$$\tilde{\Omega}_i = \bigcup_{k=1}^{\lfloor \tilde{L}_i/2 \rfloor} \left[k\frac{2\pi}{\tilde{L}_i} - \tilde{L}_i \omega_s, \min\left(k\frac{2\pi}{\tilde{L}_i} + \tilde{L}_i \omega_s, \pi \right) \right]. \qquad (10c)$$

If $G_i(\omega)$ is determined to satisfy (10), then the resulting periodic response $G_i(\tilde{L}_i \omega)$ provides the desired attenuation for the overall response $H(\omega)$ on the region

$$\Omega_i = \bigcup_{k=1}^{\lfloor \tilde{L}_i/2 \rfloor} \left[k\frac{2\pi}{\tilde{L}_{i+1}} - \omega_s, \min\left(k\frac{2\pi}{\tilde{L}_{i+1}} + \omega_s, \frac{\pi}{\tilde{L}_i} \right) \right] \qquad (11a)$$

where

$$\tilde{L}_{K+1} = L \qquad (11b)$$

and the other $\tilde{L}_i$'s are given by (4b). Each one of the subfilters $G_i(z^{\tilde{L}_i})$ concentrates on providing the desired attenuation on a certain set of the stopbands of the overall multiband stopband region Ω_s. As an example, Fig. 2 gives the partial responses for the case with $K = 3$, $L = 18$, $L_1 = 3$, and $L_2 = 3$ ($\tilde{L}_1 = 1, \tilde{L}_2 = 3, \tilde{L}_3 = 9$). Because of the periodicity, the response $G_K(\tilde{L}_K \omega)$ gives the desired attenuation, in addition to the region Ω_K, also elsewhere[4]

[2] We note that $F(z^l)$ and $G(z)$ have the common scaling constant. Therefore, we can, without loss of generality, scale $G(\omega)$ to have the value unity at $\omega = 0$.

[3] Because of the effect of $G(\omega)$, the stopband attenuation of the overall amplitude response $H(\omega)$ becomes higher on the extra stopbands of $F(L\omega)$ than on $[\omega_s, \pi/L]$.

[4] Due to of the effects of $G_i(\tilde{L}_i \omega)$, $i = 1, 2, \cdots, K-1$, the attenuation of the overall filter is higher on the extra stopbands of $G_K(\tilde{L}_K \omega)$.

except for those stopbands which are centered at the points where the response has "extra" passbands. This occurs at the points $\omega = k \cdot 2\pi/\tilde{L}_K$ for $k = 1, 2, \cdots, \lfloor \tilde{L}_K/2 \rfloor$ (at $\omega = 2\pi/9, 4\pi/9, 6\pi/9, 8\pi/9$ in Fig. 2). Similarly, $G_{K-1}(\tilde{L}_{K-1} \omega)$ takes care of the remaining stopbands except for the ones centered at the extra passband of this stage, i.e., at $\omega = k \cdot 2\pi/\tilde{L}_{K-1}$ for $k = 1, 2, \cdots, \lfloor \tilde{L}_{K-1}/2 \rfloor$ (at $\omega = 2\pi/3$ in Fig. 2). Finally, $G_1(\omega)$ provides the desired attenuation on the stopbands centered at $\omega = k \cdot 2\pi/\tilde{L}_2$ for $k = 1, 2, \cdots, \lfloor \tilde{L}_2/2 \rfloor$ (at $\omega = 2\pi/3$ in Fig. 2).

C. The Design Algorithm

The design of $F(z)$ satisfying (6) can be performed directly by using the following error function in the arbitrary magnitude FIR filter design program of McClellan et al. [14]:

$$E_F(\omega) = W_F(\omega)[F(\omega) - D_F(\omega)] \qquad (12a)$$

where the desired function $D_F(\omega)$ and the weight function $W_F(\omega)$ are

$$D_F(\omega) = \begin{cases} \dfrac{1}{G(\omega/L)} & \text{for } \omega \in [0, L\omega_p] \\ 0 & \text{for } \omega \in [L\omega_s, \pi] \end{cases} \qquad (12b)$$

$$W_F(\omega) = \begin{cases} G(\omega/L) & \text{for } \omega \in [0, L\omega_p] \\ \dfrac{\delta_p}{\delta_s} G(\omega/L) & \text{for } \omega \in [L\omega_s, \pi]. \end{cases} \qquad (12c)$$

The above error function has been chosen in such a way that both the passband specifications of (7a) and the stopband specifications of (7b) are just met when the peak absolute error is equal to δ_p. Therefore, the order of $F(z)$ has to be selected to make the peak absolute error less than or equal to δ_p. Similarly, the desired $G_i(\omega)$'s can be found using the same program with the error functions given by

$$E_i(\omega) = W_i(\omega)[G_i(\omega) - D_i(\omega)] \qquad (13a)$$

where

$$D_i(\omega) = \begin{cases} 1, & \text{for } \omega \in [0, \epsilon] \\ 0, & \text{for } \omega \in \tilde{\Omega}_i \end{cases} \qquad (13b)$$

$$W_i(\omega) = \begin{cases} \alpha, & \text{for } \omega \in [0, \epsilon] \\ F\left(\dfrac{L\omega}{\tilde{L}_i} \right) \prod_{\substack{k=1 \\ k \ne i}}^{K} G_k\left(\dfrac{\tilde{L}_k \omega}{\tilde{L}_i} \right), & \text{for } \omega \in \tilde{\Omega}_i. \end{cases} \qquad (13c)$$

By selecting ϵ to be a very small number and α to be very large, this error function forces $G_i(\omega)$ to take the value 1 at $\omega = 0$.[5] The specifications of (10) are met if the peak absolute value of the above error function is less than or equal to δ_s.

[5] When a very small value of ϵ is used, the program of McClellan et al. uses only one grid point in the passband. Therefore, there is only one extremum (of value 1) in the passband.
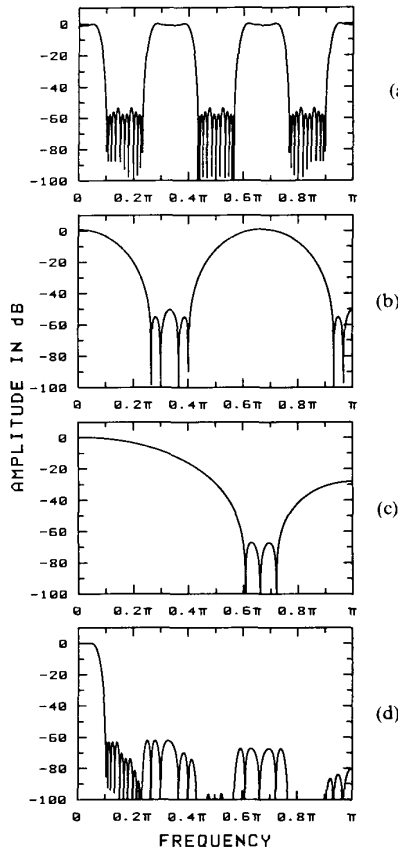
Fig. 3. Design of an optimum IFIR filter with two-stage $G(z)$ meeting the criteria: $\omega_p = 0.05\pi$, $\omega_s = 0.1\pi$, $\delta_p = 0.01$, $\delta_s = 0.001$. $L = 6$, $L_2 = 3$, $N_F = 17$, $N_{G_1} = 6$, $N_{G_2} = 4$. (a) $F(L\omega)$. (b) $G_2(\tilde{L}_2\omega)$. (c) $G_1(\omega)$. (d) Overall filter.

The steps in the algorithm for simultaneously designing $F(z^L)$ and the subfilters $G_i(z^{L_i})$ (for given filter orders) are as follows:

1) Set $F(\omega) \equiv 1$ and $G_i(\omega) \equiv 1$, $i = 1, 2, \cdots, K$.
2) Determine successively $G_i(\omega)$, $i = 1, 2, \cdots, K$, to minimize the maximum absolute value of $E_i(\omega)$ on $[0, \epsilon] \cup \tilde{\Omega}_i$.
3) Determine $F(\omega)$ to minimize the maximum absolute value of $E_F(\omega)$ on $[0, L\omega_p] \cup [L\omega_s, \pi]$.
4) Repeat steps 2 and 3 until the difference between successive overall solutions is within the given tolerance limits.

The above algorithm starts by initializing the amplitude responses of the subfilters. Then, the subfilters $G_i(z^{L_i})$ are determined successively, using the remaining amplitude responses as a weighting function, such that the corresponding error function $E_i(\omega)$ is minimized. At each stage, $E_i(\omega)$ becomes equiripple on $\tilde{\Omega}_i$ with the maximum number of oscillation around zero subject to the condition $G(0) = 1$. This condition binds one degree of freedom. The maximum number of oscillations around zero on $\tilde{\Omega}_i$ is thus $\lfloor N_{G_i}/2 \rfloor + 1$. After applying step 2) $F(z^L)$ is determined to give the desired equiripple behavior for the overall re-

sponse on $[0, \omega_p] \cup [\omega_s, \pi/L]$. The number of alternating extrema is $\lfloor N_F/2 \rfloor + 2$ as for conventional minimax FIR designs.

At this point, the error functions $E_i(\omega)$ have no longer the desired equiripple nature because of the change in the subfilters designed after $G_i(z^{L_i})$. Therefore, step 2 is repeated. After that, $F(z^L)$ is redesigned to compensate for the changes caused by the new subfilters $G_i(z^{L_i})$. The resulting $F(z^L)$ does not differ much from the previous one and as the algorithm proceeds, two consecutive $F(z^L)$'s approach each other. The same is true for the subfilters $G_i(z^{L_i})$. Typically, three to five iterations of the whole algorithm are required to arrive at the desired solution.

The resulting overall amplitude response $H(\omega)$ has an equiripple behavior on $[0, \omega_p] \cup [\omega_s, \pi/L]$ and on each one of the regions Ω_i, $i = 1, 2, \cdots, K$. This is exemplified in Fig. 3 for a filter with $K = 2$. (For this filter, $L = 6$,
$L_2 = 2$, $\tilde{L}_1 = 1, \tilde{L}_2 = 3$, $[0, \omega_p] \cup [\omega_s, \pi/L] = [0, 0.05\pi] \cup [0.1\pi, \pi/6]$. $\Omega_2 = [\pi/3 - 0.1\pi, \pi/3]$ and $\Omega_1 = [2\pi/3 - 0.1\pi, 2\pi/3 + 0.1\pi]$.) Because each one of these regions is primarily shaped by an individual filter, the ripples on the regions differ slightly from each other. The final parameters to be determined are the minimum subfilter orders to meet the given criteria. The optimality of the resulting solutions with respect to the number of multipliers is considered in Appendix A. In addition, it is shown that by making the ripples equal, the largest ripple decreases only very slightly. The algorithm of this section gives thus a good enough solution and a further optimization is not worth doing. Good estimates for the minimum subfilter orders are given in the nest section.

III. PROPERTIES OF OPTIMAL IFIR FILTERS

In this section, optimal decompositions of IFIR filters are discussed for both single-stage and multistage implementations of $G(z)$. In addition, it is shown how the minimum subfilter orders can be estimated very accurately. With the estimated values, it is possible to find a nearly optimum decomposition. Furthermore, the effects of finite wordlength are considered and compared to those of conventional direct-form designs.

A. Optimal Decompositions

To illustrate the dependence of the optimal filter decomposition on the stopband edge angle as well as on the relative transition bandwidth of the filter, we have considered the following four cases:

Case I: $\omega_p = 0.05\pi$, $\omega_s = 0.1\pi$, $\delta_p = 0.01$, $\delta_s = 0.001$
Case II: $\omega_p = 0.09\pi$, $\omega_s = 0.1\pi$, $\delta_p = 0.01$, $\delta_s = 0.001$
Case III: $\omega_p = 0.01\pi$, $\omega_s = 0.02\pi$, $\delta_p = 0.01$, $\delta_s = 0.001$
Case IV: $\omega_p = 0.018\pi$, $\omega_s = 0.02\pi$, $\delta_p = 0.01$, $\delta_s = 0.001$

Fig. 4 shows the total multiplier requirements in these four cases to implement $G(z)$, $F(z^L)$, and the overall filter as a function of L for the single-stage implementation of $G(z)$. The case $L = 1$ corresponds to the optimal direct form FIR filter. In these comparisons, the symmetry in filter coefficients has been exploited. As seen from the figure, the IFIR filters provide significant reductions in the
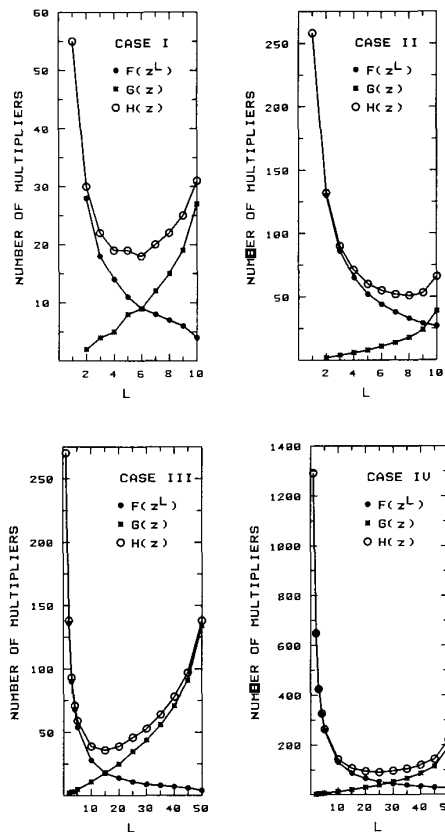
Fig. 4. Plots of the number of multipliers versus L for the shaping filter $F(z^L)$, the interpolator $G(z)$, and the overall filter $H(z)$.

Fig. 5. The ratio of the overall order of the new filter to that of the conventional direct-form minimax design.

number of multipliers over equivalent optimal direct-form designs. Savings of the same order are obtained also in the number of adders. The price paid for these reductions is a slight increase in the number of delay elements, as shown in Fig. 5.

As shown in Fig. 4, the number of multipliers of $F(z^L)$ decreases approximately exponentially and that of $G(z)$ increases exponentially as L increases. The minimum of the total number of multipliers is obtained by increasing L until the decrease in the number of multipliers of $F(z^L)$ becomes smaller than the increase in the number of multipliers of $G(z)$. The minimum value of the total number of multipliers occurs well below the theoretical upper limit $L_{max} = \lfloor \pi/\omega_s \rfloor$. When comparing the curves for Cases I, II, III, and IV with each other, it is observed that as the relative transition bandwidth is made smaller while keeping the stopband edge the same, the ratio of the optimum value L_{opt} of L to L_{max} becomes larger. This is because the relative contribution of $F(z^L)$ to the total multiplier requirements becomes larger. The larger value of L_{opt} results in larger savings in the number of multipliers and adders. As the stopband edge angle is decreased while keeping the relative transition bandwidth the same, the relative contribution of $G(z)$ becomes larger and L_{opt}/L_{max} decreases. However, the absolute value of L_{opt} increases, resulting in larger savings in the number of arithmetic operations.
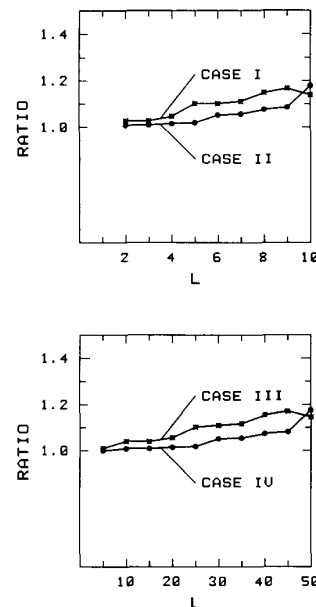
It is interesting to observe from Fig. 4 that the plot of total number of multipliers versus L is flat around $L = L_{opt}$.[6] This means that optimizing the overall multiplier requirements for $L = iK$ with K being a small integer results in a nearly optimum solution. It is also interesting to observe that the plot of overall multiplier requirements versus L is unimodal[7] (see Fig. 4). This fact simplifies considerably the workload needed to identify the true minimum. In the next subsection, it is shown how the subfilter orders can be rather accurately estimated. With these estimated values, it is possible to find out the estimated optimum value of L which is in the close neighborhood of L_{opt}.

The optimum decompositions for each of the four cases for single-stage, two-stage, and three-stage implementations of $G(z)$ are given in Tables I–IV. In the cases where the same minimum number of multipliers is obtained with different decompositions, the one having the fewest number of delay elements has been selected. Table V gives, in Case IV, the optimum decompositions for two-stage designs of $G(z)$ for various values of $\tilde{L}_2$. It is observed that the overall number of multipliers does not depend critically on the selection of the value of $\tilde{L}_2$. In addition, it is seen that the total number of multipliers as a function of $\tilde{L}_2$ is again unimodal. Table VI, in turn, gives the decompositions for various values of L for a fixed value of $\tilde{L}_2$. As seen from this table, N_{G_1} remains the same independent of the value of L and the overall multiplier requirements as a function of L behaves as that for a single stage

[6] We note that in Cases III and IV the minimum number of multipliers are obtained at various values of L. In Case III, the minimum value is obtained with $L = 14, 15, 16$, and 17 and in Case IV with $L = 22, 23, 24$, and 25.

[7] This has been true in all cases considered so far.

TABLE I
COMPARISON BETWEEN OPTIMAL IFIR FILTERS AND CONVENTIONAL DIRECT-FORM FILTERS IN CASE I

	Direct-Form FIR	One-Stage $G(z)$	Two-Stage $G(z)$	Three-Stage $G(z)$
L $\tilde{L}_i$'s $(\tilde{L}_1 = 1)$	$L = 1$	$L = 6$	$L = 6$ $\tilde{L}_2 = 3$	$L = 8$ $\tilde{L}_2 = 2$ $\tilde{L}_3 = 4$
Orders	$N = 108$	$N_F = 17$ $N_{G_1} = 17$	$N_F = 17$ $N_{G_1} = 6$ $N_{G_2} = 4$	$N_F = 12$ $N_{G_1} = 3$ $N_{G_2} = 4$ $N_{G_3} = 5$
Number of Multipliers	55	18	16	15
Number of Adders	108	34	27	24
Number of Delay Elements	108	119	120	127
Saving over Direct-Form Design	1.00	3.06	3.44	3.67

TABLE II
COMPARISON BETWEEN OPTIMAL IFIR FILTERS AND CONVENTIONAL DIRECT-FORM FILTERS IN CASE II

	Direct-Form FIR	One-Stage $G(z)$	Two-Stage $G(z)$	Three-Stage $G(z)$
L $\tilde{L}_i$'s $(\tilde{L}_1 = 1)$	$L = 1$	$L = 8$	$L = 9$ $\tilde{L}_2 = 3$	$L = 8$ $\tilde{L}_2 = 2$ $\tilde{L}_3 = 4$
Orders	$N = 515$	$N_F = 65$ $N_{G_1} = 34$	$N_F = 57$ $N_{G_1} = 7$ $N_{G_2} = 14$	$N_F = 65$ $N_{G_1} = 3$ $N_{G_2} = 4$ $N_{G_3} = 7$
Number of Multipliers	258	51	41	42
Number of Adders	515	99	78	79
Number of Delay Elements	515	554	562	559
Saving over Direct-Form Design	1.00	5.06	6.29	6.00

TABLE III
COMPARISON BETWEEN OPTIMAL IFIR FILTERS AND CONVENTIONAL DIRECT-FORM FILTERS IN CASE III

	Direct-Form FIR	One-Stage $G(z)$	Two-Stage $G(z)$	Three-Stage $G(z)$
L $\tilde{L}_i$'s $(\tilde{L}_1 = 1)$	$L = 1$	$L = 12$	$L = 28$ $\tilde{L}_2 = 7$	$L = 36$ $\tilde{L}_2 = 6$ $\tilde{L}_3 = 18$
Orders	$N = 535$	$N_F = 44$ $N_{G_1} = 25$	$N_F = 18$ $N_{G_1} = 12$ $N_{G_2} = 11$	$N_F = 14$ $N_{G_1} = 10$ $N_{G_2} = 6$ $N_{G_3} = 5$
Number of Multipliers	270	36	23	21
Number of Adders	535	69	41	35
Number of Delay Elements	535	553	593	640
Saving over Direct-Form Design	1.00	7.50	11.74	12.86

TABLE IV
COMPARISON BETWEEN OPTIMAL IFIR FILTERS AND CONVENTIONAL DIRECT-FORM FILTERS IN CASE IV

	Direct-Form FIR	One-Stage $G(z)$	Two-Stage $G(z)$	Three-Stage $G(z)$
L $\tilde{L}_i$'s $(\tilde{L}_1 = 1)$	$L = 1$	$L = 24$	$L = 40$ $\tilde{L}_2 = 8$	$L = 45$ $\tilde{L}_2 = 5$ $\tilde{L}_3 = 15$
Orders	$N = 2580$	$N_F = 106$ $N_{G_1} = 71$	$N_F = 65$ $N_{G_1} = 17$ $N_{G_2} = 21$	$N_F = 57$ $N_{G_1} = 9$ $N_{G_2} = 6$ $N_{G_3} = 14$
Number of Multipliers	1291	80	53	46
Number of Adders	2580	177	103	86
Number of Delay Elements	2580	2615	2785	2819
Saving over Direct-Form Design	1.00	16.14	24.36	28.07

implementation of $G(z)$ as a function of L. The above facts can be exploited in searching for the optimum solutions for multistage implementations of $G(z)$.

When comparing single-stage and multistage implementations of $G(z)$ given in Tables I–IV, it is observed that, in Cases I and II, the two-stage implementation provides only a slight saving over its one-stage equivalent. This is because for the single-stage implementation the order of $G(z)$ is already very small. In Cases III and IV, the saving is significant. This is because for the two-stage implementation, $G(z)$ requires considerably fewer multipliers and the optimum decomposition occurs at a higher value of L, thus decreasing the number of multipliers of $F(z^L)$.

B. Order Estimation

For the order of $F(z^L)$ in z^L, a good estimate is

$$N_F = N/L \qquad (14)$$

where N is the minimum order of an optimum direct-form design to meet the given overall criteria.[8] This is because the order of a linear phase FIR filter is roughly inversely proportional to the transition bandwidth of the filter and the transition bandwidth for $F(z)$ is N times that for the direct-form design. This can be seen by comparing the composite filter specifications of (6) and the specifications for $F(z)$ as given by (7).

In Appendix B, a very fast and simple procedure is described for estimating the orders of the subfilters $G_i(z^{L_i})$ very accurately. This procedure is based on the use of Chebyshev polynomials of the first kind. Considerable

[8] If the order of the direct-form design is so high that the FIR filter design program of McClellan et al. [14] cannot be used for determining the minimum order, an estimate for it can be obtained using the formula given in [2].

TABLE V
OPTIMAL DECOMPOSITIONS IN CASE IV FOR TWO-STAGE DESIGNS
OF $G(z)$ FOR VARIOUS VALUES OF $\tilde{L}_2$

	L	Orders	Number of Multipliers	Number of Delays
$\tilde{L}_2 = 4$	$L = 36$	$N_F = 72$, $N_{G_1} = 6$, $N_{G_2} = 34$	59	2734
$\tilde{L}_2 = 5$	$L = 40$	$N_F = 65$, $N_{G_1} = 9$, $N_{G_2} = 34$	56	2779
$\tilde{L}_2 = 6$	$L = 36$	$N_F = 72$, $N_{G_1} = 12$, $N_{G_2} = 22$	56	2736
$\tilde{L}_2 = 7$	$L = 42$	$N_F = 64$, $N_{G_1} = 14$, $N_{G_2} = 27$	55	2891
$\tilde{L}_2 = 8$	$L = 40$	$N_F = 65$, $N_{G_1} = 17$, $N_{G_2} = 21$	53	2785
$\tilde{L}_2 = 9$	$L = 45$	$N_F = 57$, $N_{G_1} = 20$, $N_{G_2} = 24$	53	2801
$\tilde{L}_2 = 10$	$L = 40$	$N_F = 65$, $N_{G_1} = 22$, $N_{G_2} = 16$	54	2782
$\tilde{L}_2 = 11$	$L = 44$	$N_F = 61$, $N_{G_1} = 25$, $N_{G_2} = 19$	54	2918
$\tilde{L}_2 = 12$	$L = 48$	$N_F = 57$, $N_{G_1} = 28$, $N_{G_2} = 23$	56	3040

TABLE VI
OPTIMAL DECOMPOSITIONS OF IN CASE IV FOR TWO-STAGE
DESIGNS OF $G(z)$ FOR VARIOUS VALUES OF $\tilde{L}_2 = 5$

	N_{G_1}	N_{G_2}	N_F	Number of Multipliers
$L = 10$	9	3	258	137
$L = 15$	9	7	171	96
$L = 20$	9	11	128	76
$L = 25$	9	15	102	65
$L = 30$	9	20	87	60
$L = 35$	9	26	74	57
$L = 40$	9	34	65	56
$L = 45$	9	45	57	58
$L = 50$	9	77	53	71

TABLE VII
ESTIMATED AND ACTUAL ORDERS FOR TWO-STAGE DESIGNS OF
$G(z)$ FOR VARIOUS VALUES OF L

	Estimated Orders in Case III (in Case I)	Actual Orders in Case III (in Case I)	Estimated Orders in Case IV (in Case II)	Actual Orders in Case IV (in Case II)
$L = 5$	$N_F = 108$, $N_{G_1} = 8$	$N_F = 107$, $N_{G_1} = 8$	$N_F = 515$, $N_{G_1} = 8$	$N_F = 514$, $N_{G_1} = 9$
$L = 10$ ($L = 2$)	$N_F = 54$, $N_{G_1} = 19$ ($N_{G_1} = 3$)	$N_F = 54$, $N_{G_1} = 20$ ($N_{G_1} = 3$)	$N_F = 258$, $N_{G_1} = 20$ ($N_{G_1} = 3$)	$N_F = 258$, $N_{G_1} = 22$ ($N_{G_1} = 3$)
$L = 15$ ($L = 3$)	$N_F = 36$, $N_{G_1} = 33$ ($N_{G_1} = 6$)	$N_F = 35$, $N_{G_1} = 34$ ($N_{G_1} = 6$)	$N_F = 172$, $N_{G_1} = 36$ ($N_{G_1} = 6$)	$N_F = 171$, $N_{G_1} = 38$ ($N_{G_1} = 7$)
$L = 20$ ($L = 4$)	$N_F = 27$, $N_{G_1} = 50$ ($N_{G_1} = 9$)	$N_F = 26$, $N_{G_1} = 48$ ($N_{G_1} = 9$)	$N_F = 129$, $N_{G_1} = 54$ ($N_{G_1} = 10$)	$N_F = 128$, $N_{G_1} = 57$ ($N_{G_1} = 11$)
$L = 25$ ($L = 5$)	$N_F = 22$, $N_{G_1} = 68$ ($N_{G_1} = 13$)	$N_F = 21$, $N_{G_1} = 68$ ($N_{G_1} = 14$)	$N_F = 103$, $N_{G_1} = 76$ ($N_{G_1} = 15$)	$N_F = 102$, $N_{G_1} = 75$ ($N_{G_1} = 15$)
$L = 30$ ($L = 6$)	$N_F = 18$, $N_{G_1} = 88$ ($N_{G_1} = 18$)	$N_F = 17$, $N_{G_1} = 87$ ($N_{G_1} = 17$)	$N_F = 86$, $N_{G_1} = 100$ ($N_{G_1} = 20$)	$N_F = 87$, $N_{G_1} = 102$ ($N_{G_1} = 20$)
$L = 35$ ($L = 7$)	$N_F = 15$, $N_{G_1} = 112$ ($N_{G_1} = 22$)	$N_F = 14$, $N_{G_1} = 111$ ($N_{G_1} = 22$)	$N_F = 74$, $N_{G_1} = 133$ ($N_{G_1} = 27$)	$N_F = 74$, $N_{G_1} = 131$ ($N_{G_1} = 26$)
$L = 40$ ($L = 8$)	$N_F = 13$, $N_{G_1} = 140$ ($N_{G_1} = 28$)	$N_F = 12$, $N_{G_1} = 141$ ($N_{G_1} = 28$)	$N_F = 64$, $N_{G_1} = 175$ ($N_{G_1} = 35$)	$N_F = 65$, $N_{G_1} = 170$ ($N_{G_1} = 34$)
$L = 45$ ($L = 9$)	$N_F = 12$, $N_{G_1} = 172$ ($N_{G_1} = 34$)	$N_F = 10$, $N_{G_1} = 180$ ($N_{G_1} = 36$)	$N_F = 57$, $N_{G_1} = 235$ ($N_{G_1} = 47$)	$N_F = 57$, $N_{G_1} = 226$ ($N_{G_1} = 46$)
$L = 50$ ($L = 10$)	$N_F = 11$, $N_{G_1} = 209$ ($N_{G_1} = 42$)	$N_F = 7$, $N_{G_1} = 266$ ($N_{G_1} = 53$)	$N_F = 52$, $N_{G_1} = 342$ ($N_{G_1} = 69$)	$N_F = 53$, $N_{G_1} = 386$ ($N_{G_1} = 77$)

TABLE VIII
ESTIMATED OPTIMAL DECOMPOSITIONS IN CASE IV FOR
TWO-STAGE DESIGNS OF $G(z)$ FOR VARIOUS VALUES OF $\tilde{L}_2$

	L	Orders	Number of Multipliers
$\tilde{L}_2 = 4$	$L = 36$	$N_F = 72$, $N_{G_1} = 6$, $N_{G_2} = 35$	59
$\tilde{L}_2 = 5$	$L = 40$	$N_F = 65$, $N_{G_1} = 8$, $N_{G_2} = 35$	56
$\tilde{L}_2 = 6$	$L = 42$	$N_F = 61$, $N_{G_1} = 10$, $N_{G_2} = 33$	54
$\tilde{L}_2 = 7$	$L = 42$	$N_F = 61$, $N_{G_1} = 13$, $N_{G_2} = 28$	53
$\tilde{L}_2 = 8$	$L = 40$	$N_F = 65$, $N_{G_1} = 15$, $N_{G_2} = 22$	53
$\tilde{L}_2 = 9$	$L = 45$	$N_F = 57$, $N_{G_1} = 18$, $N_{G_2} = 26$	53
$\tilde{L}_2 = 10$	$L = 40$	$N_F = 65$, $N_{G_1} = 20$, $N_{G_2} = 18$	54
$\tilde{L}_2 = 11$	$L = 44$	$N_F = 59$, $N_{G_1} = 23$, $N_{G_2} = 21$	53
$\tilde{L}_2 = 12$	$L = 48$	$N_F = 54$, $N_{G_1} = 26$, $N_{G_2} = 26$	56

experience with this procedure shows that it gives an estimate which differs from the actual one typically less than 3 percent. Also, the estimated value of N_F is typically within these limits.

These facts are illustrated in Tables VII and VIII. The former table compares the actual and estimated subfilter orders for a single-stage implementation of $G(z)$ for various values of L. In Case I both the estimated and actual values of N_F for a given value of L are the same as in Case III for $5L$. The same is true for Cases II and IV. This is because the passband and stopband edge angles in Case III (Case IV) are obtained by dividing the Case I (Case II) values by 5 so that the specifications for the shaping filter in Case III (Case IV) for $L = 5K$ are practically the same as in Case I (Case II) for $L = K$. The values of N_{G_1} and L given in the parentheses in Table VII are for Cases I and II. As seen from the table, the difference between the actual and estimated filter orders is very small up to $L = 45$ ($L = 9$) in Cases III and IV (I and II). The filters for $L = 50$ ($L = 10$) have the maximum value of L and they correspond to the decimators and interpolators considered in [15]. For these filters, the role of $F(z^L)$ is totally different. It concentrates only on the passband shaping, whereas $G(z)$ concentrates on shaping the stopband.

Therefore, the proposed estimation procedure does not apply very well in these cases.

Table VIII, in turn, gives the best estimated filter decompositions in Case IV for two-stage implementations of $G(z)$ for various values of $\tilde{L}_2$. For each value of $\tilde{L}_2$ given in the table, all admissible[9] values of L have been checked with the estimated subfilter orders and the one giving the smallest number of multipliers has been selected. When comparing Table VIII with Table V, it is observed that only in one case[10] the estimated orders give a non-optimum value for L. This comparison shows also that, for cases where the estimated optimum value L is the true optimum, also the estimated subfilter orders are near the optimum ones.

The above comparisons show that with the estimated subfilter orders we can find the value of L (and the values of $\tilde{L}_i$'s for a multistage implementation of $G(z)$) which is at least in a near neighborhood of the actual optimum value. After obtaining the best estimated values, the final optimization can be done using the guidelines given in Section III-A.

C. Design Examples

To illustrate the use of the estimated values together with the design algorithm of the previous section, we give some examples. As a first example, we consider the design of a Case II filter with a single-stage implementation of $G(z)$. The estimated best decomposition is $L = 8$, $N_F = 65$, and $N_{G_1} = 35$. With these values, the stopband ripples of $F(z^L)$ and $G(z)$ become $0.899\delta_s$ and $0.727\delta_s$, respectively. Therefore, the specifications may be met with lower orders. By decreasing both orders by 2, the ripples become $1.15\delta_s$ and $1.17\delta_s$. Thus these orders are too low. With $N_F = 64$ and $N_{G_1} = 34$, we obtain $1.11\delta_s$ and $0.925\delta_s$. This shows that $N_F = 64$ is too low. Hence, $N_F = 65$ and $N_{G_1} = 34$ are the minimum orders to meet the specifications. The resulting ripples are $0.890\delta_s$ and $0.926\delta_s$ (see Fig. 6(a)). If it is desired to check whether this solution is the best one with respect to the number of multipliers, it should be checked whether $L = 9$ or $L = 7$ gives a better result (recall from Section III-A that the total number of multipliers has been observed to be a unimodal function of L). If so, L should be increased or decreased until no improvement is obtained. In this example, the estimated orders give directly the optimum value of L. When comparing the above stopband ripples, it is observed that increasing one of the subfilter orders, while keeping the other one fixed, only slightly increases the ripple of the subfilter with fixed order. This shows that the minimization of the orders of $F(z^L)$ and $G(z)$ can be done rather independently.

As a second example, we consider Case IV with a two-stage $G(z)$. As seen from Table VIII, for the estimated orders, $\tilde{L}_2 = 7$, $L = 42$; $\tilde{L}_2 = 8$, $L = 40$; $\tilde{L}_2 = 9$,

[9] $L = r \cdot \tilde{L}_2$ where r is an integer

[10] This occurs for $\tilde{L}_2 = 6$. If $L = 42$, instead of $L = 36$ which gives the optimum result with actual subfilter orders, is used, only one more multiplier is required.
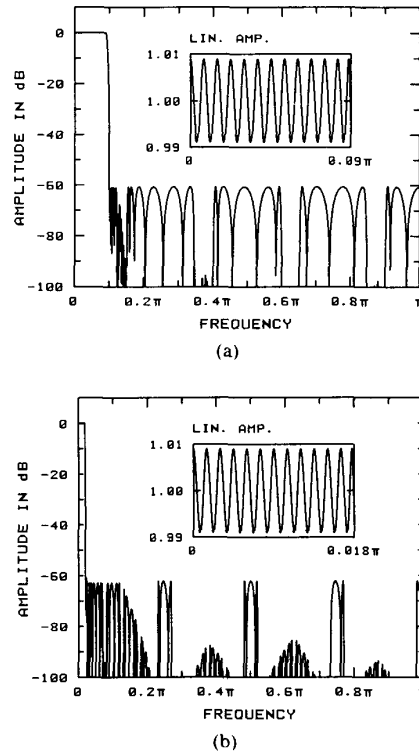
Fig. 6. Design examples. (a) Case II filter with one-stage $G(z)$. $L = 8$, $N_F = 65$, $N_{G_1} = 34$. (b) Case IV filter with two-stage $G(z)$. $L = 40$, $\tilde{L}_2 = 8$, $N_F = 65$, $N_{G_1} = 17$, $N_{G_2} = 21$.

$L = 45$; and $\tilde{L}_2 = 11$, $L = 44$ give the minimum number of multipliers. If we are interested only in a nearly optimum solution, any pair of these values can be selected. In this case, the orders of only one decomposition has to be minimized. From Tables IV and V, it is seen that the filter with actual minimum subfilter orders requires, in the worst case, at most two multiplier more than the optimum solution (obtained either with $\tilde{L}_2 = 8$, $L = 40$ or $\tilde{L}_2 = 9$, $L = 45$). Let us consider the case $\tilde{L}_2 = 8$, $L = 40$. With the estimated orders $N_F = 65$, $N_{G_1} = 15$, and $N_{G_2} = 22$, the stopband ripples on $[\omega_s, \pi/L]$, Ω_1, and Ω_2 become $0.91\delta_s$, $2.32\ \delta_s$, and $0.54\delta_s$, respectively. Therefore, N_{G_1} has to be increased and N_F and N_{G_2} might be decreased. With $N_F = 64$, $N_{G_1} = 16$, and $N_{G_2} = 21$, the stopband ripples become $1.11\delta_s$, $1.16\delta_s$, and $0.72\delta_s$, respectively. Thus $N_F = 65$ is the minimum order for $F(z^L)$, whereas N_{G_1} is still too low and N_{G_2} might be decreased. By increasing N_{G_1} by one and decreasing N_{G_2} by one, the resulting ripples on Ω_1 and Ω_2 are $0.78\delta_s$ and $1.04\delta_s$. These ripples shows that the minimum values of N_{G_1} and N_{G_2} to meet the given criteria are 17 and 21, respectively. With the minimum subfilter orders, the stopband ripples become $0.90\delta_s$, $0.78\delta_s$, and $0.71\delta_s$, respectively (see Fig. 6(b)).

If the truly optimum decomposition is desired, the next step is to check, using the estimated subfilter orders as a starting point, whether $L = 4 \cdot \tilde{L}_2 = 32$ or $L = 6 \cdot \tilde{L}_2 = 48$ gives a better result than $L = 5 \cdot \tilde{L}_2 = 40$. Recall from Section III-A that the overall number of multipliers is in

TABLE IX
Effects of Finite Wordlength on Optimal IFIR Filters and
Conventional Direct-Form Filters

	Noise Gain, Case A	Noise Gain, Case B	Number of Coefficient Bits	Number of Leading Zeros
Case I:				
Direct-Form	17.4	0.00	14	3
One-Stage $G(z)$	10.0	0.44	12	1,2
Two-Stage $G(z)$	7.5	1.17	13	1,1,2
Case II:				
Direct-Form	24.1	0.00	16	3
One-Stage $G(z)$	13.3	0.45	14	2,1
Two-Stage $G(z)$	25.8	11.51	14	1,-2,2
Case III:				
Direct-Form	24.3	0.00	13	6
One-Stage $G(z)$	11.5	0.22	14	2,7
Two-Stage $G(z)$	8.9	0.49	12	1,2,2
Case IV:				
Direct-Form	31.1	0.00	NA	NA
One-Stage $G(z)$	15.8	0.16	15	1,8
Two-Stage $G(z)$	10.3	0.43	13	2,1,3

general a unimodal function of admissible values of L for a fixed value of $\tilde{L}_2$. The following step is to find the optimal decomposition for $\tilde{L}_2 = 7$ and $\tilde{L}_2 = 9$ as for $\tilde{L}_2 = 8$ and to decrease or increase $\tilde{L}_2$ until no decrease in the overall number of multipliers occurs (The overall number of multipliers is a unimodal function of $\tilde{L}_2$ when for each $\tilde{L}_2$ the optimal decomposition is used.)

As a final example, we consider Case IV with a three-stage design of $G(z)$. With the estimated orders, the best design is obtained with $L = 45$, $\tilde{L}_2 = 5$, $\tilde{L}_3 = 15$. The estimated filter orders are $N_F = 57$, $N_{G_1} = 8$, $N_{G_2} = 6$, $N_{G_3} = 16$. As seen from Table IV, the estimated subfilter orders give directly the optimum values of L, $\tilde{L}_2$, and $\tilde{L}_3$. Also N_F and N_{G_2} are the optimum one, whereas N_{G_1} is too low by one and N_{G_3} is too high by two.

D. Effects of Finite Wordlength

To illustrate the effects of finite wordlength on IFIR filters, Table IX compares IFIR filters with one-stage and two-stage $G(z)$ to direct-form designs, in terms of output noise gain.[11] In addition, the comparison is made in terms of the number of bits required by the filter coefficients to keep the overall amplitude response within the tolerances to be given later on in this subsection. The output noise gain is given in two cases. In Case A rounding is performed after each multiplication, whereas in Case B rounding is performed at the output of each filter section. For IFIR filters, the scaling was performed according to the L_∞ norm and the filter sections were implemented in the order $F(z^L)$, $G_K(z^{L_K}), \cdots, G_1(z)$. As seen from the table,

the noise gains are lower for IFIR filters in Case A, except for the Case II IFIR filter with two-stage $G(z)$.[12] The reduction is within 7–21 dB corresponding to a 1–3 bit reduction in the required data wordlength. In Case B, the noise gains of IFIR filters are very slightly larger.

The number of bits required by the filter coefficients were determined such that the deviation from the infinite-precision design is less than 0.000112 in the stopband. This corresponds to a 1-dB deviation from the infinite-precision design in the case where the stopband attenuation is exactly 60 dB. The sign bit is included in the number of bits. If all the filter (subfilter) coefficients possess the same number of leading zeros, they are excluded from the number of bits. Again L_∞ scaling was used and the subfilter $F(z^L)$ was implemented first followed by $G_K(z^{L_K})$. The number of leading zeros given in the table follows this ordering. As seen from the table, in most cases the IFIR filters require fewer bits. The reduction becomes larger if the leading zeros are not taken into account.

IV. IFIR Filters with Recursive Running Sum Interpolators

So far the interpolator $G(z)$ is assumed to have been implemented in the conventional linear phase direct form. In this section, we show how the total number of multipliers as well as the number of adders can be further reduced by developing filter structures that more efficiently provide the desired attenuation on the region Ω_s.

A. Proposed Filter Structure

A good candidate for such a structure is to combine recursive running sum (RRS) filters with the aid of a few tap coefficients and extra delay terms, as proposed in [6], [13]. The use of recursive running sums (RRS) in implementing FIR filters has been studied extensively in [6]–[8, 16]. In [7], [8], these filters are used as prefilters. In [6], the filters are used as basic building blocks in implementing the overall filter, whereas in [16] they are used in implementing efficient early stages for sampling rate alteration.

The RRS filter can produce several zeros at equal distances without any multipliers. However, the available stopband attenuation is only moderate in the cases where rather wide regions around these zero locations are desired to be supressed. To overcome the limitations of the RRS's, we propose the use of interpolated FIR filter structures of the type (3) where the interpolator $G(z)$ can be expressed as

$$G(z) = 2^{-P_1}[R_{kL}(z)]'\prod_{r=1}^{M}\left[R_{kL}^2(z) - \delta_r z^{-(kL-1)}\right] \quad (15a)$$

where

$$R_{kL}(z) = 2^{-P_2}\frac{1 - z^{-kL}}{1 - z^{-1}}. \quad (15b)$$

---

[11] By the output noise gain we refer to the roundoff noise power at the output in reference to a unit noise source.

[12] In this case, $G_2(z^{L_2})$ contains rather large coefficients amplifying the noise produced by the filter $F(z^L)$.
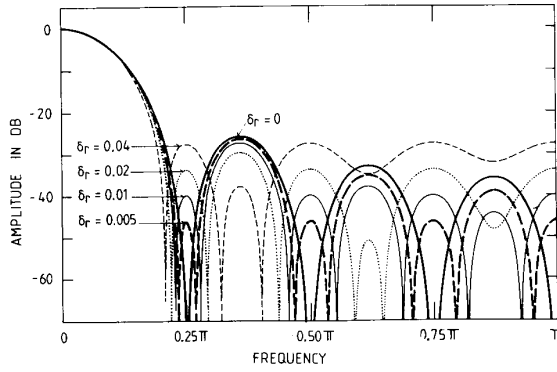
Fig. 7.   Frequency responses of $R_{kL}^2(z) - \delta_r z^{(kL-1)}$ for different values of δ_r. $L = 8$ and $k = 1$.
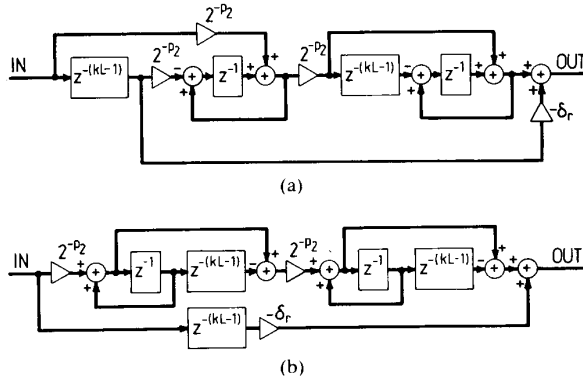

(a)

(b)

Fig. 8.   Implementations of the term $R_{kL}^2(z) - \delta_r z^{-(kL-1)}$.

Here k and l are integers and 2^{-P_1} and 2^{-P_2} are scaling constants. l or M may also be zero. Since the order of $R_{kL}^2(z)$ in (15) is $2(kL - 1)$, the use of the delay terms $z^{-(kL-1)}$ makes the overall response linear phase.

If $k = 1$, $R_{kL}(z)$ produces one zero at each one of the centers $\omega = r \cdot 2\pi/L$, $r = 1, 2, \cdots, \lfloor L/2 \rfloor$, of the unwanted passbands of $F(z^L)$. If $\delta_r = 0$ in the term $R_{kL}^2(z) - \delta_r z^{-(kL-1)}$, the term produces double zeros at these points (see Fig. 7). With increasing δ_r, these zeros separate and move away from the center frequencies. Since the ripples of $R_{kL}^2(z)$ are different in the stopband region, the movement is different around each center frequency. By appropriately determining the δ_r's, we can effectively attenuate the unwanted passbands. In [17], it is shown how the optimization of δ_r's can be converted into another approximation problem to which the Remez multiple exchange algorithm is directly applicable.

Fig. 8 gives two implementations of the term $R_{kL}^2(z) - \delta_r z^{-(kL-1)}$. The first implementation requires $2kL$ delay elements and the second one $3kL - 1$ delay elements. We note that if 1's or 2's complement arithmetic (or modulo arithmetic in general) is used and L_∞ scaling (corresponds to the worst case scaling in this case) is used, the output of the implementation of Fig. 8(b) is correct even though there may occur internal overflows. In the case of Fig. 8(a) there are no internal overflows. The implementation of Fig. 8(b) is very attractive as in this case the system does

not need initial resetting and as the effect of temporary miscalculations vanishes automatically from the output in a finite time. The above facts are explained in Appendix C.

B. Optimal Decomposition

Table X gives the optimal decompositions in Cases I–IV for $k = 1$ and $k = 2$. The number of delay elements required by equivalent direct-form designs are given in the parentheses for comparison purposes. The decompositions have been determined such that the overall number of multipliers is minimized. It has been assumed that the implementation of the RRS interpolator requires M multipliers and l in (15) is either zero or one. In the case where the same number of multipliers is obtained with different decompositions, the one having the lowest number of delay elements has been selected. In additions, it has been assumed that the term $R_{kL}^2(z) - \delta_r z^{-(kL-1)}$ is implemented as shown in Fig. 8(a) and a possible term $R_{kL}(z)$ is implemented with kL delay elements. When comparing Table X with Tables I–IV, it is seen that IFIR filters with RRS interpolator provide significantly more savings in the number of multipliers than the optimal IFIR designs at the expense of an increased number of delay elements.

As seen from Table X, the optimal decompositions are obtained with values of L which are very near the maximum allowable value $L_{\max} = \lfloor \pi/\omega_s \rfloor$ (10 for Cases I and II and 50 for Cases III and IV). Figs. 9 and 10 show the amplitude responses for the overall Case I filters with $k = 1$ and $k = 2$ as well as the amplitude responses for the subfilters. In the case $k = 2$, $G(z)$ also contributes to the attenuation outside the regions of the unwanted passbands, decreasing the order of $F(z^L)$.

It is interesting to observe from Table X that the optimal filters for Cases II and IV have the same number of multipliers. The only difference is that the values of L for the Case IV designs are obtained by multiplying the values
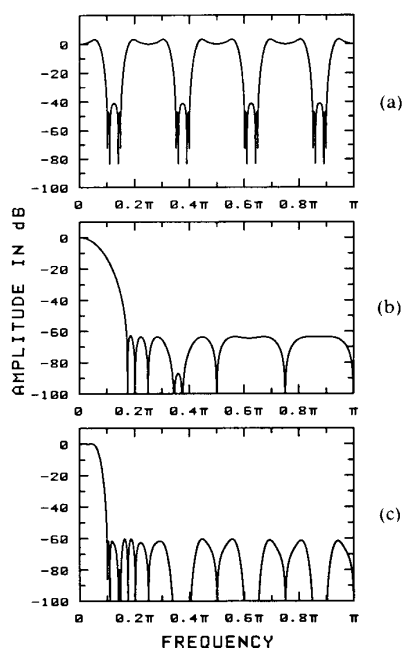
TABLE X
OPTIMAL IFIR FILTERS WITH RRS INTERPOLATOR

	L	Orders	Number of Multipliers	Number of Delay Elements	Saving over Direct-form Design
Case I with k = 1	L = 8	$N_F = 12$ $M = 2$ $l = 1$	9	136 (108)	6.11
Case I with k = 2	L = 7	$N_F = 11$ $M = 2$ $l = 0$	8	133 (108)	6.88
Case II with k = 1	L = 9	$N_F = 59$ $M = 4$ $l = 1$	34	612 (515)	7.59
Case II with k = 2	L = 8	$N_F = 61$ $M = 3$ $l = 1$	34	600 (515)	7.59
Case III with k = 1	L = 46	$N_F = 9$ $M = 3$ $l = 1$	8	736 (538)	30.00
Case III with k = 2	L = 41	$N_F = 7$ $M = 2$ $l = 1$	6	697 (538)	45.00
Case IV with k = 1	L = 45	$N_F = 59$ $M = 4$ $l = 1$	34	3060 (2580)	37.94
Case IV with k = 2	L = 40	$N_F = 61$ $M = 3$ $l = 1$	34	3000 (2580)	37.94

Fig. 9. Amplitude responses for a Case I IFIR filter with RRS interpolator with $L = 8$ and $k = 1$. (a) $F(z^L)$ of order 12. (b) $G(z)$ with $M = 2$ and $l = 1$. (c) Overall filter.
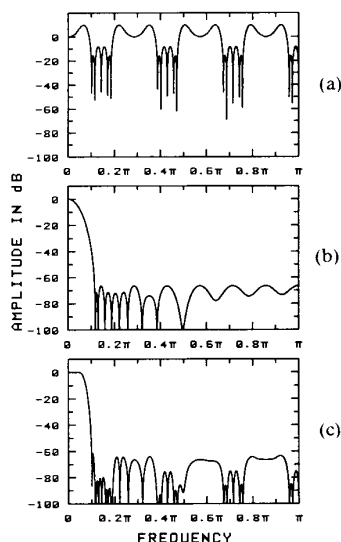

Fig. 10. Amplitude responses for a Case I IFIR filter with RRS interpolator with $L = 7$ and $k = 2$. (a) $F(z^L)$ of order 11. (b) $G(z)$ with $M = 2$ and $l = 0$. (c) Overall filter.

for the Case II designs by 5. Recall that the specifications of Case IV are obtained by dividing the edge angles of the Case II specifications by 5. This fact is also valid in general. If the edge angles of a low-pass design are divided by an integer, a filter meeting the resulting specifications is obtained by keeping the filter orders the same and by simply multiplying the L of the original design by this integer. The resulting design is a good candidate for the true optimum solution. However, since for the new specifi-

cations there are relatively much more values of L available, the resulting design is not necessarily the best one, as can be seen by comparing the Case I and Case III designs with each other.

C. Order Estimation

For $k = 1$, the order of $F(z^L)$ can be estimated as in the case of the optimum interpolator. For the number of RRS's, $2M + l$, a good estimate can be obtained using the fact that the lower limit for $2M + l$ is the order of the optimum $G(z)$ divided by $L - 1$. Usually, the minimum value of $2M + l$ is the second or the third integer which is larger than this number. For instance, in Case III the minimum values of $F(z^L)$ and $G(z)$ for the optimum IFIR filter with $L = 46$ are 9 and 192. By dividing 192 by 45 we obtain 4.2. The minimum value of $2M + l$ is 7, as seen from Table X. The minimum order of $F(z^L)$ remains the same. The resulting RRS $G(z)$ requires only 3 multipliers, whereas the optimum $G(z)$ requires 97 multipliers. The price paid for this reduction is the increase of the order of $G(z)$ from 192 to 315.

For $k = 2$, the value of $2M + l$ can be estimated in a similar manner. Since in this case $G(z)$ also contributes to the attenuation outside Ω_s, the order of $F(z^L)$ is lower than that of the optimum IFIR filter. For instance, in Case III with $L = 41$ the orders of $F(z^L)$ and $G(z)$ for the optimum IFIR filter are 12 and 148. The minimum value of $2M + l$ and the minimum order of $F(z^L)$ to meet the criteria are 5 and 7, respectively. The resulting RRS IFIR filter requires 6 multipliers, whereas the optimum IFIR filter requires 82 multipliers. The price paid for this reduction is the increase of the overall filter order from 640 to 692.

V. Design of Other Types of Filters

The above discussion was concentrated on the design of narrowband lowpass filters. This section shows how the proposed approach can be applied equally well to the design of other types of filters.

A. Design of Wideband Filters and High-Pass Filters

The design of a wideband low-pass filter can be accomplished with the aid of a narrow-band low-pass filter based on the fact that if a narrow-band filter of even order N, $H'(z)$, has the edge angles of $\omega_p' = \pi - \omega_s$ and $\omega_s' = \pi - \omega_p$ and the passband and stopband ripples of $\delta_p' = \delta_s$ and $\delta_s' = \delta_p$, then

$$H(z) = z^{-N/2} - H'(-z) \qquad (16)$$

has the edge angles of ω_p and ω_s and the passband and stopband ripples of δ_p and δ_s. The only restriction in designing the narrow-band prototype filter is that it has to be of even order.

The design of highpass filter can be based on the fact that if a lowpass filter $H'(z)$ has the edge angles of $\omega_p' = \pi - \omega_p$ and $\omega_s' = \pi - \omega_s$ and the passband and stopband ripples of $\delta_p' = \delta_p$ and $\delta_s' = \delta_s$, then $H(z) = H'(-z)$ has the edge angles of ω_p and ω_s and the passband and

stopband ripples of δ_p and δ_s. Based on this fact, we can design both narrow-band and wideband high-pass filters.

B. Design of Bandpass and Bandstop Filters

To illustrate the applicability of the proposed approach for synthesizing bandpass and bandstop filters, we consider the design of a complementary bandpass–bandstop filter pair with at least 60-dB stopband attenuations. The passband edge angles for the bandpass filter are $\omega_{p1}, \omega_{p2} = 0.7\pi \pm 0.04\pi$ and the stopband edge angles are $\omega_{s1}, \omega_{s2} = 0.7\pi \pm 0.06\pi$. The desired filter pair is obtained by designing a bandpass filter of even order and having the passband and stopband ripples of at most 0.001. If $H(z)$ is the transfer function of the bandpass filter of even order N, then the complementary bandstop filter is $z^{-N/2} - H(z)$.

The minimum even-order of a direct-form minimax design to meet the given bandpass filter specifications is 336, requiring 169 multipliers. In the IFIR approach, the number of multipliers is minimized by using $L = 5$. The given criteria are met with $N_F = 68$ and $N_{G_1} = 32$. This filter requires 52 multipliers, providing a saving by a factor of 3.25 over the direct-form minimax design. In this case, $F(z^L)$ takes care of shaping the passband and of primarily providing the desired attenuation on the regions $[0.6\pi, \omega_{s1}]$ and $[\omega_{s2}, 0.8\pi]$ (see Fig. 11), whereas $G(z)$ attenuates to the desired level the unwanted passbands and transition bands of $F(z^L)$. The design of the overall filter can be done by slightly modifying the design algorithm of Section II-C. $G(z)$ can be designed by forcing $G(\omega)$ to go through the value 1 at the passband center frequency and by simultaneously minimizing $F(L\omega)G(\omega)$ on those regions where $F(L\omega)$ has the undesired passbands and transition bands. Because of the periodicity of the response $F(L\omega)$, its design can be done most conveniently on the region $[0, \pi/L]$. Using the transformation $\omega \mapsto 4\pi/L - \omega$, the approximating function becomes $F(L\omega)G(4\pi/L - \omega)$ ($F(L(4\pi/L - \omega) = F(L\omega)$) and the resulting passband and stopband edge angles in the region $[0, \pi/L]$ are obtained from the original ones using the given transformation.

Generally, useful values of L for designing bandpass IFIR filters are those for which there exist an integer r such that $\omega_{s1}, \omega_{s2} \in [r\pi/L, (r+1)\pi/L]$. For these values of L, the design of $G(z)$ can be accomplished as in the previous example. The design of $F(z^L)$ can be transformed onto the interval $[0, \pi/L]$ by using the transformation

$$\omega \mapsto h(\omega) \tag{17a}$$

where

$$h(\omega) = \begin{cases} \omega - r\pi/L, & \text{for } r \text{ even} \\ (r+1)\pi/L - \omega, & \text{for } r \text{ odd}. \end{cases} \tag{17b}$$

The resulting approximation function is[13] $F(L\omega)G(h(\omega))$ and the edge angles are obtained from the original ones using the transformations of (17). The remaining problem is to determine L such that the given criteria are met with

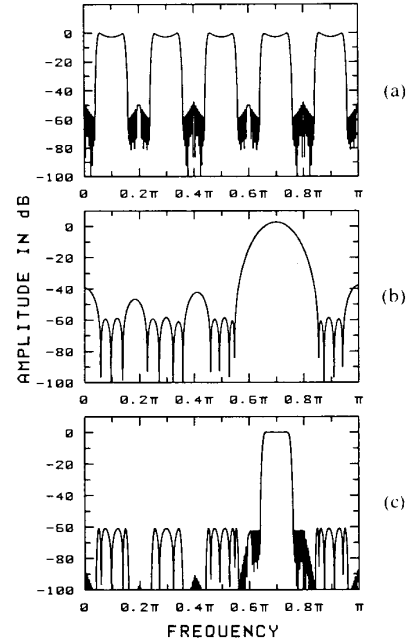[13] Because of the periodicity. $F(Lh(\omega)) = F(L\omega)$.

Fig. 11. Design of an optimum bandpass IFIR filter with one-stage $G(z)$ meeting the criteria: $\omega_{p1}, \omega_{p2} = 0.7\pi \pm 0.04\pi$, $\omega_{s1}, \omega_{s2} = 0.7\pi \pm 0.06\pi$, $\delta_p = \delta_s = 0.001$. $L = 5$, $N_F = 68$, $N_{G_1} = 32$. (a) $F(L\omega)$. (b) $G(\omega)$. (c) Overall filter.

the minimum number of multipliers, as in the low-pass designs.

VI. COMPARISON WITH OTHER DESIGNS

We now compare the proposed IFIR filters with other multiplier efficient FIR designs. The comparison is made only with the designs whose structures are predetermined to provide a significant reduction in the number of arithmetic operations compared to direct-form designs.

A. Filters of Jing and Fam

To compare the new filters with the filters of Jing and Fam [11], we have designed a filter meeting the Case I specifications using their approach. The optimum solution is obtained with $M = 3$, $n_1 = n_2 = 2$, $\alpha_1 = \alpha_2 = 1$, $N_1 = 6$, $N_2 = 7$, $N_3 = 27$. This filter requires 22 multipliers, whereas the best new design with optimum interpolator requires 15 multipliers and the new design with RRS interpolator requires 8 multipliers. Fig. 12 shows plots of the overall number of multipliers versus the stopband edge angle ω_s for filters with $\delta_p = 0.01$, $\delta_s = 0.001$, and $\omega_p = \omega_s/2$. Case I and Case III designs are special cases in these plots. The plots are given for direct-form designs, the optimized new designs with optimum and RRS interpolators, and for optimized Jing–Fam designs. As seen from the figure, the Jing–Fam designs require approximately 40 percent more multipliers than the new design with optimum interpolator. It is also interesting to observe that the new design with optimum interpolator is better than the direct-form design even for $\omega_s = 0.4\pi$. This shows that the proposed approach can equally well be used for designing rather
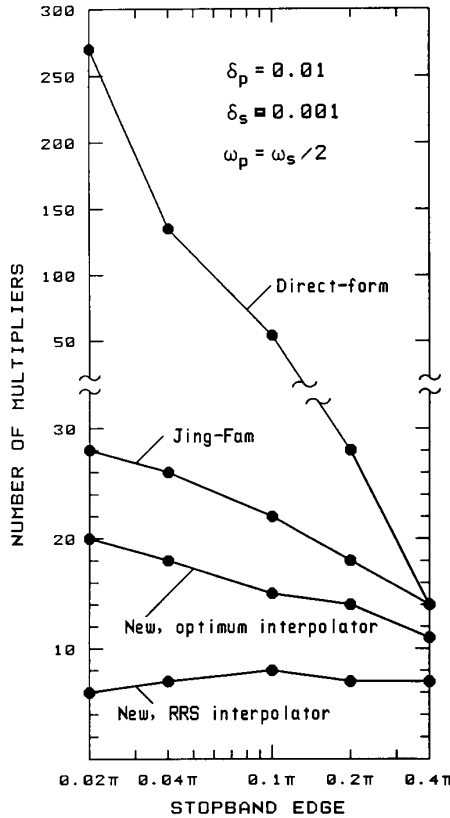
Fig. 12. Plots of the required number of multipliers versus the stopband edge angle ω_s. $\omega_p = \omega_s/2$, $\delta_p = 0.01$, $\delta_s = 0.001$.

wideband filters. As explained in Section IV-B, the number of multipliers of the proposed design with RRS interpolator remains approximately the same as ω_p and ω_s are divided by the same number. Therefore, this design becomes better compared to the Jing–Fam design as ω_s is made smaller.

B. Filters of Adams and Willson

To compare the new filters with the filters of Adams and Willson, we have designed the new filter meeting the criteria given in [8]: $\omega_p = 0.042\pi$, $\omega_s = 0.14\pi$, $\delta_p = 0.0115$, $\delta_s = 0.001$. These specifications are met with $L = 6$, $M = 2$, $l = 0$, $k = 2$, and $F(z^L)$ of order 5. The above criteria can be met by a small number of arithmetic operations since the specifications have been selected such that the relative transition band is very wide. The new filter requires 5 general multipliers, 15 adders, and 78 delay elements. The corresponding numbers for the best filter of Adams and Willson are 17, 37, and 73. The proposed design provides thus a saving by a factor of 3.4 in the number of multiplier.

C. Filters of Boudreaux and Parks

We consider the specifications [5]: $\delta_p = 0.009$, $\delta_s = 0.0193$, $\omega_p = 0.002\pi$, $\omega_s = 0.05\pi$. These criteria can be met by using only the interpolator $G(z)$ and no shaping filter

$F(z^L)$ is needed. The specifications are met by an RRS interpolator with $L = 27$, $k = 1$, $M = 1$, and $l = 1$. This interpolator has been designed to take care of the overall stopband shaping. Because of a very narrow passband region, the passband specifications are automatically satisfied. The resulting overall filter requires one δ_s-multiplier and a multiplier to give the passband average of unity. The overall number of multipliers is thus two. The Boudreaux–Parks design requires 14 multipliers so that a saving by a factor of 7 is provided by the new design in the number of multipliers. The price paid for this saving is a slight increase in the order of the overall filter (64 compared to 78). It should be noted that the given criteria can be also met by simply cascading three pure running sums with $L = 31$ and $k = 1$. In this case, the overall filter order is 90.

D. Filters of Chu and Burrus

We consider the specifications [10]: $\delta_p = 0.114$, $\delta_s = 0.033$, $\omega_p = 0.02\pi$, $\omega_s = 0.04\pi$. These specifications are met by an IFIR filter with a RRS interpolator with $L = 18$, $N_F = 5$, $k = 1$, $M = 1$, and $l = 1$. This filter requires 4 multipliers and the overall filter length is 141. The equivalent Chu–Burrus filter designed in [10] requires 7 multipliers and the overall filter length is 198. The proposed design provides, in the number of multipliers, a saving by a factor of 1.75.
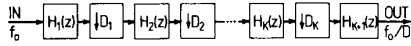
E. Filters of Saramäki

In [13], Saramäki has designed a filter meeting the Case I specifications with 4 very simple multipliers (sums or differences of two powers-of-two), which is half of that one of the best IFIR filter (cf. Table X). The number of adders and the overall filter length for the IFIR filter are 21 and 129, respectively, whereas the corresponding values for the Saramäki design are 27 and 184. Thus the IFIR filter has a lower filter length at the expense of an increased number of multipliers.

F. Filters Based on Decimator Designs

It is well known (see, e.g., [15]) that if FIR filters designed for decimation purposes are implemented without sampling rate alteration, we obtain implementations which provide significant savings over direct-form designs in terms of the overall number of multipliers. Fig. 13 shows the most general implementation form [17] for a decimator in the case where the overall sampling rate conversion ratio can be factored into the product

$$D = \prod_{k=1}^{K} D_k \qquad (18)$$

where D_k's are integers. By substituting $F(z) = H_{K+1}(z)$ and $L_k = D_k$ and $G_k(z) = H_k(z)$ for $k = 1, 2, \cdots, K$, the transfer function of the corresponding single-stage implementation can be written exactly in the form of (3) and (4). In the case of conventional FIR decimators [18], [19], the last stage $H_{K+1}(z)$ is absent. In this case, the transfer

Fig. 13. A general implementation form for a D-to-1 decimator.

function can be expressed in the form of (3) and (4) by substituting $F(z) = H_K(z)$ and $L_k = D_k$ and $G_k(z) = H_k(z)$ for $k = 1, 2, \cdots, K-1$ and finally by substituting $K - 1 \mapsto K$. The basic difference between the most general decimator transfer functions and the transfer functions of the proposed designs is that for the decimator design ω_s and L are related via $\omega_s = \pi/L$ so that L is restricted to be the largest possible $L_{\max} = \pi/\omega_s$. For conventional FIR decimators, L is restricted to be an integer fraction of $L_{\max}$ to make the factorization of $L_{\max}$ possible.

If the don't care bands considered in [19] are used, the conventional two-stage FIR decimator meets the Case I specifications with $L = 5$, $N_F = 24$, $N_G = 21$. This corresponds to factorizing the overall sampling rate conversion ratio $D = 10$ into $D_1 = 5$ and $D_2 = 2$, which gives the best result. The resulting single-rate design requires 25 multipliers, whereas the best new design with one-stage optimum interpolator requires only 18 multipliers. Another advantage of the new design compared to the conventional decimator design is that for the new design we can use multistage $G(z)$. For the conventional decimator design, only the factorizations $D_1 = 2$, $D_2 = 5$ and $D_1 = 5$, $D_2 = 2$ so that only two subfilters can be used. With a three-stage $G(z)$, the overall number of multipliers of the new design can further be reduced to 15.

The basic difference between the above decimator filter and the new filter with a single-stage $G(z)$ designed for $L = 5$ is that for the decimator design both $F(z^L)$ and $G(z)$ are designed separately, whereas for the new design they are determined simultaneously. This reduces the order of $G(z)$ from 24 to 14 (cf. Table VII). The order of $F(z^L)$ is the same for both designs.

The best generalized FIR decimated design [17] (having the last stage of Fig. 13) meets the Case I specifications with $K = 2$, $L = 10$, $\tilde{L}_2 = 5$, $N_F = 7$, $N_{G_1} = 13$, and $N_{G_2} = 9$. The resulting single-rate design requires one multiplier more (16 multipliers) than the best new design with optimum interpolator. This design is a special case of the proposed filters. The best generalized FIR decimator for $K = 1$ is obtained with $L = 10$, $N_F = 13$, $N_G = 38$. This filter is obtained by properly overdesigning $F(z^L)$. The resulting filter requires considerably more multipliers than the new design with a single-stage $G(z)$ (27 compared to 18).

G. Filters with Lth-Band Interpolators

One alternative to construct an efficient interpolator $G(z)$ is to use Lth-band filters [20] or a cascade of Lth-band filters as proposed in [21] by the authors. The advantage of these designs is that they simultaneously take care of passband shaping and every Lth impulse response value, except for the central value, are zero. Especially for half-band filters, approximately half of the impulse re-

sponse values are zeros and the central impulse response value has an easily implementable value of $1/2$. However, these interpolators require more multipliers for reasons shown below.

Multistage Lth-band filters considered in [21] have the transfer function which are exactly of the same form as that for $G(z)$ as given by (4). The program described in [21] can be used for simultaneously optimizing the subfilters such that the overall filter provides the desired attenuation on Ω_s as given by (8). Because of the properties of Lth-band filters, the resulting filter has automatically a good passband behavior. The remaining problem is then to design the shaping filter to meet (7). The best filter to meet the Case I specifications is obtained using $K = 3$, $L = 8$, $\tilde{L}_2 = 2$, $\tilde{L}_3 = 4$. In this case, the interpolator is an eighth-band filter consisting of three halfband filters $G_i(z)$. The given criteria are met with $N_{G_1} = 6$, $N_{G_2} = 10$, $N_{G_3} = 34$, and $N_F = 12$. When comparing these orders with the orders of the new design of Table I with a three-stage interpolator, it is observed that the orders of $G_i(z^{\tilde{L}_i})$'s are significantly higher for the design with an eighth-band interpolator. The reason is that the half-band designs are forced to have some zeros for shaping the passband. These zeros decrease, in turn, the stopband attenuation so that more zeros are needed for the stopband shaping. If we assume that the central coefficient of value $1/2$ (and of course the zero-valued coefficients) are implemented without general multipliers, the overall design with eighth-band interpolator requires 21 general multipliers. This is six more than that for the proposed design. Also the overall number of delay elements is considerably higher (258 compared to 127).

H. Multirate Implementations

In [22], Rabiner and Crohiere have designed a low-pass filter as a cascade of a decimator and an interpolator to meet the Case I specifications. When both the decimator and interpolator are single-stage designs, the resulting overall filter requires 18.4 multiplications per input sample. The corresponding optimum IFIR filter with single-stage $G(z)$ requires 18 multiplications per input sample (cf. Table I) so that the multiplication rates for both of these designs are about the same. The delay and the number of distinct multipliers of the proposed single-stage design are lower (59.5 samples compared to 120 samples and 18 multipliers compared to 61 multipliers). Also the number of delay elements required in the implementation is lower (119 compared to 240). The corresponding multirate filter with two-stage decimator and interpolator requires slightly less multiplications per input sample than the optimum IFIR filter with two-stage $G(z)$ (11.7 compared to 16). The price paid for this reduction is the increase in the overall filter delay (158 compared to 60) and in the number of distinct multipliers (27 compared to 16). The number of required delay elements is slightly lower for the multirate implementation (100 compared to 120).

VII. CONCLUSIONS

In this paper two methods for designing efficient FIR filters with same input and output rates were presented. In the first method, the shaping filter $F(z^L)$ and the interpolator $G(z)$ of the IFIR filter structure were simultaneously optimized with a method based on the Remez multiple exchange algorithm. The design examples and comparisons with other efficient methods indicate that the method is quite efficient in terms of the number of multipliers, multiplication rate, number of adders, number of delays and signal propagation delay. The main reason why the method is efficient even if compared with transfer functions designed for decimator purposes and multirate structures is that the shaping filter and the interpolator can be optimized simultaneously for an optimal overall performance without any concern of internal aliasing errors.

In the second method, an efficient interpolator was derived which further reduced the number of arithmetic operations required in the IFIR implementation. The method utilized the fact that the unwanted passbands of the shaping filter $F(z)$ are equally spaced and zeros on them can be placed by suitably simultaneously displacing the zeros of two running sums with a single multiplier. The examples indicate that the second method is comparable in the number of multipliers to IIR structures. The number of multipliers remained essentially constant as the passband and transition bands were simultaneously made narrower. This behavior is typical to IIR structures, too.

There is no established theoretical or empirical relationship between the required number of arithmetic operations and the required number of delays for FIR filters that are noncanonical in delays. This makes it difficult to compare the efficiency of different FIR structures. However, experience shows that by increasing the number of delays the number of multipliers and adders can be decreased. The methods presented in this paper seem to be close to optimal as in addition to a small number of arithmetic operations, the number of delays is only 10–20 percent more than that in the canonical design.

In this paper we concentrated only on the design of efficient IFIR structures. There are several approaches one can take to further develop the methods. For medium wide bandwidths these IFIR based methods can be combined with the methods of Lim [23] and Jing and Fam [11]. For symmetrical bandpass filters, the approach presented in [24] gives an alternative design approach with efficient implementation and easy tuning of center frequency. This approach can use the optimal low-pass IFIR filters proposed in this paper as a starting point of the design.

APPENDIX A

The algorithm of Section II-C gives a solution where the shaping filter $F(z^L)$ provides for the overall error function

$$E(\omega) = W(\omega)[H(\omega) - D(\omega)] \qquad (A.1)$$

where

$$D(\omega) = \begin{cases} 1, & \text{for } \omega \in [0, \omega_p] \\ 0, & \text{for } \omega \in [\omega_s, \pi] \end{cases} \qquad (A.2)$$

$$W(\omega) = \begin{cases} 1, & \text{for } \omega \in [0, \omega_p] \\ \delta_p/\delta_s, & \text{for } \omega \in [\omega_s, \pi] \end{cases} \qquad (A.3)$$

$\lfloor N_F/2 \rfloor + 2$ alternating extrema of values $\pm \delta_F$ on $[0, \omega_p] \cup [\omega_s, \pi/L]$. The subfilter $G_i(z^{\tilde{L}_i})$ provides for the overall error function $\lfloor N_{G_i}/2 \rfloor + 1$ alternating extrema of values $\pm \delta_i$ on Ω_i, as given by (11). Thus the overall number of extrema on $[0, \omega_p] \cup [\omega_s, \pi/L] \cup_{i=1}^K \Omega_i$ is $\lfloor N_F/2 \rfloor + \Sigma_{i=1}^K \lfloor N_{G_i}/2 \rfloor + K + 2$. Since the subfilters have the common scaling constant, the number of adjustable variables for the overall filter is

$$N = \lfloor N_F/2 \rfloor + \sum_{i=1}^K \lfloor N_{G_i}/2 \rfloor + 1. \qquad (A.4)$$

Therefore, the solution obtained using the algorithm of Section II-C has K extrema more than that required by the equiripple solution ($N+1$). This shows that we can use K degrees of freedom for making the ripples δ_F and δ_i for $i = 1, \cdots, K$ equal and for making the overall solution equiripple with $N+1$ extrema. One possibility is to use as primary unknowns the location of the first unit-circle zero pairs of those K filter stages which provide the smallest ripples (only the filter stage whose ripple is the largest is not taken into consideration). For fixed values of these zeros, the overall filter can be determined using the algorithm of Section II-C such that the primary unknown zero locations are included in the weighting functions and the orders of the filter stages, except for that one providing the largest ripple, are decreased by two. The remaining problem is to find the unknown zero locations such that the ripples δ_F and δ_i for $i = 1, \cdots, K$ become equal.

As an example, we consider Case I with two-stage $G(z)$ ($L = 6$, $\tilde{L}_2 = 3$, $N_F = 17$, $N_{G_1} = 6$, $N_{G_2} = 4$). In this case, the original algorithm results in a solution where the attenuations provided by $F(z^L)$, $G_2(z^{\tilde{L}_1})$, and $G_1(z)$ are 63.24 dB, 62.20 dB, and 67.34 dB, respectively (cf. Fig. 3). Therefore, the first unit-circle zeros of $F(z)$ and $G_1(z)$ are selected as primary unknowns. By moving the zero of $F(z)$ from $\omega = 0.6055\pi$ to $\omega = 0.6002\pi$ and the zero of $G_1(z)$ from $\omega = 0.6082\pi$ to $\omega = 0.5885\pi$, we obtain an equiripple solution having a 62.66-dB attenuation (see Fig. 14). Thus making the ripples equal increases the lowest attenuation only by 0.46 dB, showing that in practice a further optimization is not worth doing. The price paid for this improvement is a 4.67-dB reduction on the region which is primarily shaped by $G_1(z)$.

As a second example, we consider the design of a Case I filter with a single-stage $G(z)$ ($L = 6$, $N_F = N_{G_1} = 17$). In this case $F(z^L)$ provides a 63.27-dB attenuation and $G(z)$ a 61.52-dB attenuation (see Fig. 15(a)). By moving a zero of $F(z)$ from $\omega = 0.6055\pi$ to $\omega = 0.597\pi$, we obtain an
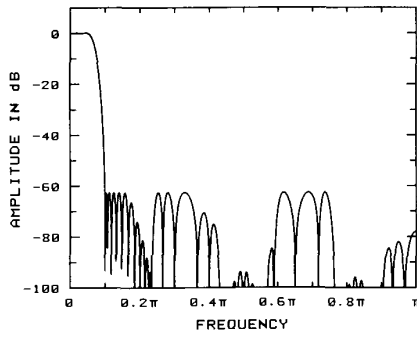
Fig. 14. Optimized Case I IFIR filter with two-stage $G(z)$. $L = 6$, $L_2 = 3$, $N_F = 17$, $N_{G_1} = 6$, $N_{G_2} = 4$.
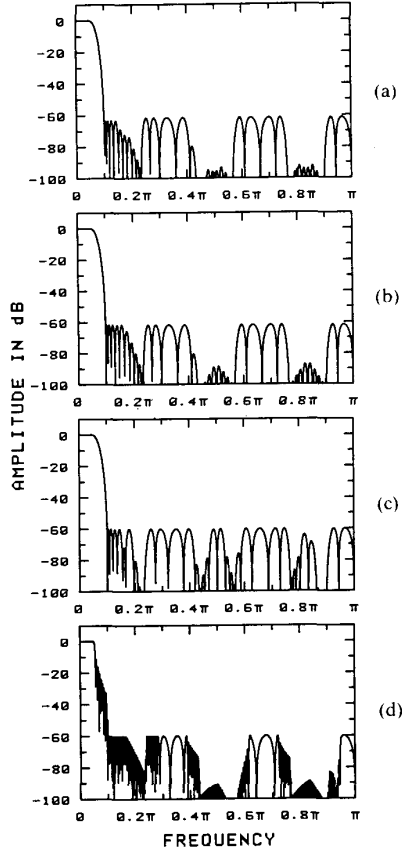

Fig. 15. Amplitude responses for Case I IFIR filters with one-stage $G(z)$ and $L = 6$. (a) Solution of the algorithm of Section II-C for $N_F = N_{G1} = 17$ (b) Optimized equiripple solution for $N_F = N_{G1} = 17$. (c) Optimized equiripple solution for $N_F = 15$. $N_{G_1} = 25$. (d) Optimized equiripple solution for $N_{G_1} = 15$. $N_F = 69$.

equiripple solution with a 61.81-dB attenuation (see Fig. 15(b)). Thus the improvement in the minimum stopband attenuation is only 0.29 dB.

Sharing the frequency response shaping responsibilities in the manner described in Section II is only one possibility. However, in all cases considered so far, this resulted in the minimum number of multipliers required in the implementation. To illustrate this, we consider Case I with single-stage $G(z)$. The proposed design is obtained with

$N_F = N_{G_1} = 17$, and $L = 6$. Figs. 15(c) and 15(d) give the responses of the optimized equiripple filters for $N_F = 15$ and for $N_{G_1} = 15$, respectively. In the former case, $N_{G_1} = 25$ is required to meet the given criteria and, in the latter case, $N_F = 69$ is required. These filters require considerably more multipliers than the original design.[14]

The design of the filter of Fig. 15(c) was performed in such a way that $F(z^L)$ provides the desired attenuation on the region $[\omega_s, \pi/L - \beta]$ $(L = 6)$. $G(z)$ provides the desired attenuation, in addition to the region Ω_s, as given by (8), also on the intervals $[(2r - 1)\pi/L - \beta, (2r - 1)\pi/L + \beta]$ for $r = 1, 2, 3$, which are not shaped by $F(z^L)$. The remaining problem is to find β in such a way that the given criteria are met with the minimum value of N_{G_1} and the resulting solution becomes equiripple (this is achieved with $\beta = 0.0214\pi$). In this case of Fig. 15(d), $G(z)$ was determined to meet the given criteria on the intervals $[2r\pi/L - \beta, \min(2r\pi/L + \beta, \pi]$ for $r = 1, 2, 3$ $(\omega_p < \beta < \omega_s)$. For $\beta < \omega_s$, $F(z^L)$ has to take care of the remaining portion of Ω_s. The extra requirements for $F(z^L)$ are most stringent on $[2\pi/L - \omega_s, 2\pi/L - \beta]$. These extra requirements can be met by including the transition band requirement

$$-\delta_s \le G(2\pi/L - \omega)F(L\omega) \le \delta_s, \quad \text{for } \omega \in [\beta, \omega_s] \tag{A.5}$$

in the design of $F(z^L)$. The equiripple solution is achieved with $\beta = 0.0477\pi$. If N_F is decreased from 17 by one, N_{G_1} has to be increased to 21, and if N_{G_1} is decreased from 17 by one, N_F has to be increased to 29.

APPENDIX B

For the orders of the subfilters $G_i(z^{L_i})$, good estimates can be obtained with the aid of FIR filters whose amplitude responses oscillate the maximum number of times within the limits $\pm \delta_s$ in the stopband $[\tilde{\omega}_{s1}, \tilde{\omega}_{s2}]$ and are uniformly decaying as ω varies from 0 to $\tilde{\omega}_{s1}$. The order of the filter taking the value 1 at $\omega = \tilde{\omega}_p < \tilde{\omega}_{s1}$ can be derived easily with the aid of the Chebyshev polynomials of the first kind in a manner similar to the derivation used for finding the formulas for the corresponding low-pass design [2]. The estimated filter order is

$$N(\tilde{\omega}_p, \tilde{\omega}_{s1}, \tilde{\omega}_{s2}, \delta_s) = \frac{2 \cosh^{-1}(1/\delta_s)}{\cosh^{-1} X(\tilde{\omega}_p, \tilde{\omega}_{s1}, \tilde{\omega}_{s2})} \tag{B.1a}$$

where

$$X(\omega, \tilde{\omega}_{s1}, \tilde{\omega}_{s2}) = \frac{2 \cos \omega - \cos \tilde{\omega}_{s1} - \cos \tilde{\omega}_{s2}}{\cos \tilde{\omega}_{s1} - \cos \tilde{\omega}_{s2}}. \tag{B.1b}$$

This filter has the response

$$T(\omega, \tilde{\omega}_p, \tilde{\omega}_{s1}, \tilde{\omega}_{s2}, \delta_s) = \delta_s \cosh\left[\frac{1}{2}N(\tilde{\omega}_p, \tilde{\omega}_{s1}, \tilde{\omega}_{s2}, \delta_s)\right.$$
$$\left. \cdot \cosh^{-1} X(\omega, \tilde{\omega}_{s1}, \tilde{\omega}_{s2})\right]. \tag{B.2}$$

[14] In the first case, 21 multipliers are required and, in the second case, 43, whereas the original design requires 18 multipliers.

An estimate for the order of $G_i(z)$ can be obtained by considering the following specifications:

$$G_i\left(\tilde{L}_i\omega_p\right) = 1 \qquad (B.3a)$$

$$-\delta_s \le G_i(\omega) \le \delta_s, \qquad \text{for } \omega \in \hat{\Omega}_i \qquad (B.3b)$$

where

$$\hat{\Omega}_i = \bigcup_{k=1}^{\lfloor L_i/2 \rfloor} [\tilde{\omega}_{2k-1}, \tilde{\omega}_{2k}] \qquad (B.3c)$$

with

$$\tilde{\omega}_{2k-1} = k\frac{2\pi}{L_i} - \tilde{L}_i\left[\omega_p + \alpha(\omega_s - \omega_p)\right] \qquad (B.3d)$$

$$\tilde{\omega}_{2k} = \min\left(k\frac{2\pi}{L_i} + \tilde{L}_i\left[\omega_p + \alpha(\omega_s - \omega_p)\right], \pi\right). \qquad (B.3e)$$

These specifications have three differences compared to the specifications of (10). First, the effects of the other subfilters are ignored. Secondly, the bandwidths of the stopbands are made smaller. This is because $F(z^L)$ takes part in providing the desired attenuation in the very beginning and in the very end of the intervals $[2k\pi/L - \omega_s, 2k\pi/L + \omega_s]$ for $k = 1, 2, \cdots, \lfloor L/2 \rfloor$ (subintervals of Ω_s as given by (8)). Finally, $G_i(\omega)$ is normalized to have the value 1 at $\omega = \tilde{L}_i\omega_p$, instead of $\omega = 0$. In this case, the resulting periodic response $G_i(\tilde{L}_i\omega)$ takes the value 1 at $\omega = \omega_p$ and provides the desired attenuation from ω_p to the corresponding stopband region.[15]

The desired estimate can be obtained using the following procedure:

1) Set $\delta_k = 1$ for $k = 1, 2, \cdots, \lfloor L_i/2 \rfloor$. Set $\omega_k^{\text{cen}} = (\tilde{\omega}_{2k-1} + \tilde{\omega}_{2k})/2$ and $N_{G_i} = 0$.

2) Determine successively

$$N_k = N\left(\tilde{L}_i\omega_p, \tilde{\omega}_{2k-1}, \tilde{\omega}_{2k}, \delta_k\right), \qquad k = 1, 2, \cdots, \lfloor L_i/2 \rfloor$$

where

$$\delta_k = \delta_s \prod_{\substack{r=1 \\ r \ne k}}^{\lfloor l_i/2 \rfloor} \frac{1}{T\left(\omega_r^{\text{cen}}, \tilde{L}_i\omega_p, \tilde{\omega}_{2r-1}, \tilde{\omega}_{2r}, \delta_r\right)}.$$

3) Evaluate

$$N_{Gi}' = \sum_{k=1}^{\lfloor L_i/2 \rfloor} N_k.$$

4) If $|N_{G_i} - N_{G_i}'| \le \epsilon$, stop. Otherwise set $N_{G_i} = N_{G_i}'$ and go to step 2.

In this algorithm, it is assumed that the overall filter is a cascade of $\lfloor L_i/2 \rfloor$ filters where the kth subfilter provides

---

[15] The desired function for $F(z^L)$, $1/G(\omega)$, is monotonously increasing in the passband. Therefore, the highest value in the passband is obtained at $\omega = \omega_p$. Because of the periodity, $F(L\omega)$ attains this value also at $\omega = 2\pi/L \pm \omega_p, 4\pi/L \pm \omega_p, \cdots$. Therefore, it is required that $G_i(\tilde{L}_i\omega)/G_i(\tilde{L}_i\omega_p)$ attains at most the specified value of δ_s at $\omega = 2k\pi/\tilde{L}_{i+1} \pm \omega_p$ for $k = 1, 2, \cdots, \lfloor L_i/2 \rfloor$ or, equivalently, $G_i(\omega)/G_i(\tilde{L}_i\omega_p)$ attains at most this value at $\omega = 2k\pi/L_i \pm \tilde{L}_i\omega_p$ for $k = 1, 2, \cdots, \lfloor L_i/2 \rfloor$.

the desired attenuation for the overall filter on the subinterval $[\tilde{\omega}_{2k-1}, \tilde{\omega}_{2k}]$. All these subfilters attain the value of 1 at $\omega = \tilde{L}_i\omega_p$. When determining for the first time the order of the first filter, the stopband ripple is initially δ_s.[16] For the other filters, the contribution of the previously determined responses are taken into account by determining the product of these responses in the middle point of the interval. δ_s is then divided by this product in order to obtain the desired overall attenuation at this point. In the following iterations, the effects of all the other responses are included. The algorithm is repeated until the sum of the orders of the subfilters remain the same. All the orders in the above algorithm are considered as real numbers. Finally, the resulting N_{G_i} is rounded to the nearest integer.

For high values of L_i ($L_i > 25$), we can utilize the fact that the order of the filter satisfying (B.3) with $L_i = rK$ is approximately K times that of the filter meeting

$$\tilde{G}_i\left(K\tilde{L}_i\omega_p\right) = 1 \qquad (B.4a)$$

$$-\delta_s \le \tilde{G}_i(\omega) \le \delta_s, \qquad \text{for } \omega \in \hat{\Omega}_i' \qquad (B.4b)$$

where

$$\hat{\Omega}_i' = \bigcup_{k=1}^{\lfloor L_i/(2K) \rfloor} [\tilde{\omega}_{2k-1}', \tilde{\omega}_{2k}'] \qquad (B.4c)$$

with

$$\tilde{\omega}_k' = \min\left(K\tilde{\omega}_k, \pi\right). \qquad (B.4d)$$

Using this fact, the orders can be estimated for values $L_i = rK$, $r = 1, 2, \cdots$. In between values can then be found using linear interpolation.

Considerable experience with the above procedure shows that by selecting α in (B.3) to be $2/3$, it gives an estimate for the subfilter order which differs from the actual one typically less than 3 percent.

APPENDIX C

The basic building block of the structure of Fig. 8(b) is shown in Fig. 16. Assuming that the initial values of the delay elements are zero, the filter is characterized in the time domain by

$$y(n) = w(n) - w(n - kL) \qquad (C.1a)$$

$$w(n) = \begin{cases} 0, & \text{for } n < 0 \\ \sum_{k=0}^{n} x(k), & \text{for } n \ge 0. \end{cases} \qquad (C.1a)$$

Calculating the output sample $y(n)$ involves thus only additions. On the other hand, 2's (or 1's) complement arithmetic has the desired property that as long as the final sum of the numbers to be added is within the range $[-1, 1)$, partial sums can overflow and still cause no problems. Therefore, if this arithmetic are used, the output

---

[16] This is achieved by setting initially $\delta_k = 1$ for $k = 1, 2, \cdots, \lfloor L_i/2 \rfloor$. This makes the orders of the $T(\cdot)$-functions for $r = 2, 3, \cdots, \lfloor L_i/2 \rfloor$ equal to zero and these functions become identically equal to 1.
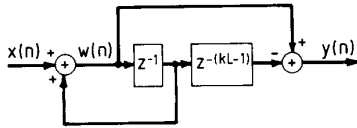
Fig. 16.   An implementation of a recursive running sum filter.

sample $y(n)$ is correct as long as

$$y(n) = w(n) - w(n - kL) = \sum_{k = \max(0, n - kL + 1)}^{n} x(k)$$

(C.2)

is within the above limits. This means that if a scaling constant whose value is less than or equal to $1/(kL)$ is used, there are no uncontrollable overflows in the structure of Fig. 16.

Let us assume that there is an initial state variable value in the feedback loop at time $n = 0$. In this case,

$$w(n) = \alpha + \sum_{k = 0}^{n} x(k)$$

(C.3)

and

$$y(n) = w(n), \quad \text{for } n < kL.$$

(C.4)

Hence, the output is not correct for $n < kL$. However, for $n \geq kL$, both $w(n)$ and $w(n - kL)$ contain the initial state variable value α and the output is as given (C.2). According to the above considerations, the output is correct if the input samples are scaled in such a way that the right-hand side of (C.2) is within the desired limits. Hence, the initial state variable value has no effect on the output value for $n \geq kL$ regardless of its value. Using a similar reasoning, it is clear that the effect of a temporary miscalculation of the state variable value vanishes from the output after kL samples. Thus there is no need for resetting the system initially or during the actual operation.

Similarly, it can be shown that the output of the structure of Fig. 8(a) is correct if a proper scaling and 1's or 2's complement arithmetic is used. In this case, initial resetting is needed.
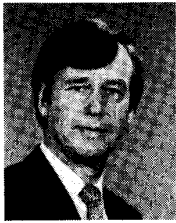
REFERENCES

[1] J. F. Kaiser, "Nonrecursive digital filter design using I_0-sinh window function," in Proc. 1974 IEEE Int. Symp. Circuits Syst., Apr. 1974, pp. 20–23; also reprinted in Digital Signal Processing II (Digital Signal Processing Committee). New York: IEEE Press, 1975, pp. 123–126.
[2] O. Herrmann, L. R. Rabiner, and D. S. K. Chan, "Practical design rules for optimum finite response lowpass digital filters," Bell Syst. Tech. J., vol. 52, pp. 769–799, July–Aug. 1973.
[3] J. F. Kaiser and R. W. Hamming "Sharpening the response of a symmetric nonrecursive filter by multiple use of the same filter," IEEE Trans. Acoust., Speech, Signal Processing, vol. ASSP-25, pp. 415–422, Oct. 1977.
[4] S. Nakamura and S. K. Mitra, "Design of FIR digital filters using tapped cascaded FIR subfilters," Circuits, Systems and Signal Processing, vol. 1, no. 1, pp. 43–56, 1982.
[5] G. F. Boudreaux and T. W. Parks, "Thinning digital filters: A piecewise-exponential approach," IEEE Trans. Acoust., Speech, Signal Processing, vol. ASSP-31, pp. 105–112, Feb. 1983.
[6] T. Saramäki, "Computationally efficient narrowband linear phase FIR filters," IEEE Proc. G, Electron Circuits and Syst., vol. 130, pp. 20–24, Feb. 1983.
[7] J. W. Adams and A. N. Willson, Jr., "A new approach to FIR digital filters with fewer multipliers and reduced sensitivity," IEEE Trans. Circuits Syst., vol. CAS-30, pp. 277–283, May 1983.
[8] ____, "Some efficient digital prefilter structures," IEEE Trans. Circuits Syst., vol. CAS-31, pp. 260–265, Mar. 1984.
[9] S. Chu and C. S. Burrus, "Efficient recursive realizations of FIR filters, Part I: The filter structures," Circuits, Systems and Signal Processing, vol. 3, no. 1, pp. 3–20, 1984.
[10] S. Chu and C. S. Burrus, "Efficient recursive realizations of FIR filters, Part II: Design and applications," Circuits, Systems and Signal Processing, vol. 3, no. 1, pp. 21–57, 1984.
[11] Z. Jing and A. T. Fam, "A new structure for narrow transition band, lowpass digital filter design" IEEE Trans. Acoust., Speech, Signal Processing, vol. ASSP-32, pp. 362–370, Apr. 1984.
[12] Y. Neuvo, C.-Y. Dong, and S. K. Mitra, "Interpolated finite impulse response filters," IEEE Trans. Acoust., Speech, Signal Processing, vol. ASSP-32, pp. 563–570, June 1984.
[13] T. Saramäki, "Design of FIR filters as a tapped cascaded interconnection of identical subfilters," IEEE Trans. Circuits Syst., Sept. 1987; a shorter version in Proc. Int. Conf. on Computers, Systems, and Signal Processing (Bangalore, India), pp. 1649–1652, Dec. 1984.
[14] J. H. McClellan, T. W. Parks, and L. R. Rabiner, "A computer program for designing optimum FIR linear phase digital filters," IEEE Trans. Audio Electroacoust., vol. AU-21, pp. 506–526, Dec. 1973.
[15] T. Saramäki, "A class of linear-phase FIR filters for decimation, interpolation, and narrow-band filtering," IEEE Trans. Acoust., Speech, Signal Processing, vol. ASSP-32, pp. 1023–1036, Oct. 1984.
[16] T. Saramäki, "Efficient recursive digital filters for sampling rate conversion," Proc. 1983 IEEE Int. Symp. Circuits Syst., (Newport Beach, CA), pp. 1322–1326, May 1983.
[17] T. Saramäki, "Design of optimal multistage IIR and FIR filters for multirate filtering—Part I: Design of decimators and interpolators; Part II: Design of narrowband filters," Proc. 1986 IEEE Int. Symp. Circuits Syst., (San Jose, CA), pp. 227–230, May 1986.
[18] R. E. Crochiere and L. R. Rabiner, "Optimum FIR digital filter implementations for decimation, interpolation, and narrowband filtering," IEEE Trans. Acoust., Speech, Signal Processing, vol. ASSP-23, pp. 444–456, Oct. 1975.
[19] R. E. Crochiere and L. R. Rabiner, "Further considerations in the design of decimators and interpolators," IEEE Trans. Acoust., Speech, Signal Processing, vol. ASSP-24, pp. 296–311, Aug. 1976.
[20] F. Mintzer, "On half-band, third-band, and Nth-band FIR filters and their design," IEEE Trans. Acoust., Speech, Signal Processing, vol. ASSP-30, pp. 734–738, Oct. 1982.
[21] T. Saramäki and Y. Neuvo, "A class of FIR Nyquist filters with zero intersymbol interference," IEEE Trans. Circuits Syst., Oct. 1987; a shorter version in Proc. International Conf. on Computers, Systems, and Signal Processing (Bangalore, India), pp. 1653–1657, Dec. 1984.
[22] L. R. Rabiner and R. E. Crochiere, "A novel implementation for narrow-band FIR digital filters," IEEE Trans. Acoust., Speech, Signal Processing, vol. ASSP-23, pp. 457–464, Oct. 1975.
[23] Y. C. Lim, "Frequency-response masking approach for the synthesis of sharp linear phase digital filters," IEEE Trans. Circuits Syst., vol. CAS-33, pp. 357–364, Apr. 1986.
[24] Y. Neuvo, G. Rajan, and S. K. Mitra, "Design of narrow-band FIR bandpass digital filters with reduced arithmetic complexity," IEEE Trans. Circuits Syst. pp. 409–419, Apr. 1987.

✳

Tapio Saramäki was born in Orivesi, Finland, on June 12, 1953. He received the degrees of Diploma Engineer (with honors) and Doctor of Technology (with honors) in electrical engineering from the Tampere University of Technology, Tampere, Finland in 1978 and 1981, respectively.

Since 1977, he has been with the Department of Electrical Engineering of the Tampere University of Technology. From 1979 to 1982, he simultaneously served as a Research Engineer for the Academy of Finland. Since 1982, he has been a Research Fellow at the same institution. In 1982, 1985, and 1986, he was a Visiting Research Scholar at the University of California, Santa Barbara. His research interests are in the areas of digital signal processing and approximation theory.

Yrjö Neuvo (S'70–M'74–SM'82) was born in Turku, Finland, in 1943. He received the Diploma Engineer and Licentiate of Technology degrees from the Helsinki University of Technology, 1968 and 1971, respectively, and the Ph.D. degree in electrical engineering from Cornell University, Ithaca, NY, in 1974.

He has held various research and teaching positions at the Helsinki University of Technology, the Academy of Finland, and Cornell University, from 1968 to 1976. Since 1976 he has been a Professor of Electrical Engineering at the Tampere University of Technology, Tampere, Finland. The academic year 1981–1982 he was with the University of California, Santa Barbara as a Visiting Professor. Since 1983 he has held the position of National Research Professor at the Academy of Finland. His main research interests are in digital signal and image processing algorithms and their implementations. He is in the General Chairman of the 1988 IEEE International Symposium on Circuits and Systems.

Dr. Neuvo is a member of Phi Kappa Phi, and the Finnish Academy of Technical Sciences.

✳

Sanjit K. Mitra (S'59–M'63–SM'69–F'74) received the B.Sc. (Hons.) degree in physics in 1953 from Utkal University, Cuttack, India; the M.Sc. (Tech.) degree in radio physics and electronics in 1956 from Calcutta University, Calcutta, India; the M.S. and Ph.D. degrees in electrical engineering from the University of California, Berkeley, in 1960 and 1962, respectively.

He was a member of the faculty of the Cornell University, Ithaca, NY, from 1962 to 1965, a member of the Technical Staff of the Bell Laboratories 1965 to 1967. He joined the faculty of the University of California, Davis in 1967, and transferred to the Santa Barbara campus in 1977 as a Professor of Electrical and Computer Engineering, where he served as Chairman of the Department from July 1979 to June 1982. He has held visiting appointments at universities in Australia, Finland, India, West Germany, and Yugoslavia.

He is the recipient of the 1973 F.E. Terman Award and the 1985 AT&T Foundation Award of the American Society of Engineering Education, a Visiting Professorship from the Japan Society for Promotion of Science in 1972, and the Distinguished Fullbright Lecturer Award for Brazil in 1984 and Yugoslavia in 1986. Dr. Mitra is a Fellow of the AAAS, and a member of the ASEE, EUROSIP, Sigma Xi, and Eta Kappa Nu. He is a member of the Advisory Council of the George R. Brown School of Engineering of Rice University, Houston, TX, and an Honorary Professor of the Northern Jiaotong University, Beijing, China. In May 1987, he was awarded an Honorary Doctorate of Technology degree from the Tampere University of Technology, Finland.